SEMMELWEIS EGYETEM

DOKTORI ISKOLA

Ph.D. értekezések

3268.

CZÁRÁN DOMONKOS TAMÁS

Celluláris és molekuláris élettan

című program

Programvezető: Dr. Hunyady László egyetemi tanár

Témavezető: Dr. Csépányi-Kömi Roland, egyetemi docens

INVESTIGATING THE ROLE OF ARHGAP25 IN INFLAMMATORY DISEASES USING MURINE MODELS

PhD thesis

Domonkos Czárán

Molecular Medicine Doctoral School

Semmelweis University

Supervisor:	Roland Csépányi-Kömi, Ph.D
Official reviewers:	László Cervenak, Ph.D Andrea Papp-Balogh, Ph.D
Head of the Complex Examination Committee:	Sára Tóth, Ph.D
Members of the Complex Examination Committee:	Éva Ruisanchez, Ph.D Dorottya Kövesdi, Ph.D

Budapest
2025

TABLE OF CONTENTS

LIST OF ABBREVIATIONS

RA	Rheumatoid arthritis
RF	Rheumatoid factor
ACPA	Anti-citrullinated protein
Th	T helper cell
Tc	Cytotoxic T cell
TNF-α	Tumor necrosis factor-α
IL	Interleukin
T_{reg}	Regulatory T cell
B_{reg}	Regulatory B cell
MMP	Matrix metalloprotease
MPO	Myeloperoxidase
ROS	Reactive oxygen species
NET	Neutrophil extracellular trap
FLS	Fibroblast-like synoviocyte
RANKL	Receptor activator of nuclear factor kappa-B ligand
ACD	Allergic contact dermatitis
DTH	Delayed-type hypersensitivity
LC	Langerhans cell
DDC	Langerin-dermal dendritic cell
TCR	T cell receptor
DETC	Dendritic epidermal T cells
IFN	Interferon

MAPK	Mitogen-activated protein kinase
NF-κB	Nuclear factor-κB
BAFF	B cell activating factor
CIA	Collagen-induced arthritis
STA	Serum transfer arthritis
TNCB	2,4,6-trinitrochlorobenzene
CHS	Contact hypersensitivity
NOD	Non-obese diabetic
ICAM-I	Adhesion molecule-1
MHC	Major histocompatibility complex
APC	Antigen-presenting cell
G6PI	Glucose-6-phosphate isomerase
IC	Immune complex
C5a	Complement component 5a
LTB	Leukotriene B
G-CSF	Granulocyte colony-stimulating factor
GM-CSF	Granulocyte-macrophage stimulating factor
GEF	Guanine nucleotide exchange factor
GAP	GTPase-activating protein
HPSC	Hematopoietic stem cell
GC	Glucocorticoid
NSAID	Nonsteroidal anti-inflammatory drug
DMARD	Disease-modifying antirheumatic drugs

mAb	Monoclonal antibody
JAK	Janus kinase
DPA	Dynamic plantar aesthesiometer
SSC	Somatosensory cortex
PAG	Periaqueductal gray matter
SC	Spinal cord
PMN	Polymorphonuclear neutrophil
HBSS	Hank’s balanced salt solution
PMA	Phorbol 12-myristate 13-acetate
FBS	Fetal bovine serum
HSA	Human serum albumin
OD	Optical density
PBS	Phosphate-buffered saline
HEPES	N’-2-hydroxyethylpiperazine-N’-2-ethanesulfonic acid
EDTA	Ethylenediaminetetraacetic acid
ELISA	Enzyme-linked immunosorbent assay
Rplp0	Ribosomal protein lateral stalk subunit p0
MIP	Macrophage inflammatory protein
WB	Western blot
RT-qPCR	Quantitative reverse transcription polymerase chain reaction
HE	Hematoxylin and eosin

1. INTRODUCTION

1.1. Rheumatoid Arthritis

Rheumatoid arthritis (RA) is one of the most common autoimmune inflammatory diseases with a prevalence of 0.5-2% in the population of the industrialized world. It is approximately twice as common in women as in men and mainly affects people over 50. It is characterized by inflammation and subsequent pain of the synovial joints (mostly small joints of the hands and feet), which, if not treated sufficiently, can progress to severe conditions with cartilage destruction and bone erosion, and even extraarticular manifestations, substantially reducing the life quality of patients (1, 2).

The cause of RA is still not fully understood. However, it is established that it requires both genetic predisposition (which can lead, for instance, to the development of autoreactive T and B cells) and environmental factors, such as infections or tissue injury, that can trigger the onset of the disease. These factors provide stimuli for the antigen-presenting cells, which in turn activate the previously formed autoreactive lymphocytes (3).

The pathogenesis of the disease results from a complex combination of factors and immunologic events involving a multitude of cells and molecules. In the preclinical phase of rheumatoid arthritis (RA), autoantibodies, known as rheumatoid factors (RF) and anti-citrullinated protein antibodies (ACPA), develop years before the onset of the first symptoms. RF is a pentameric IgM that binds to the Fc portion of IgG antibodies. In contrast, the isotype of ACPA can be IgM, IgG, or IgA and recognizes post-translationally modified (citrullinated, homo-citrullinated, and acetylated) self-proteins, for example, type II collagen, histones, fibrinogen, fibronectin, and vimentin. The development of these autoantibodies is associated with an interplay between genetic predisposition (mainly susceptibility coded in the HLA genes) and environmental factors such as smoking, periodontitis, and certain gut microbes (4). As the disease progresses, more and more autoantibodies with different specificities develop, creating a diverse pool of autoreactive antibodies in the system. This phenomenon, called epitope spreading, seems to be an essential aspect of the pre-RA phase of the disease, associated with a faster transition to the clinical RA phase when symptoms appear and develop (5).

Joint inflammation involves numerous interactions between infiltrated leukocytes, primarily T cells, B cells, monocytes, and neutrophils, and resident cells, such as chondrocytes, fibroblasts, osteoclasts, and osteoblasts (Figure 1, Figure 2).

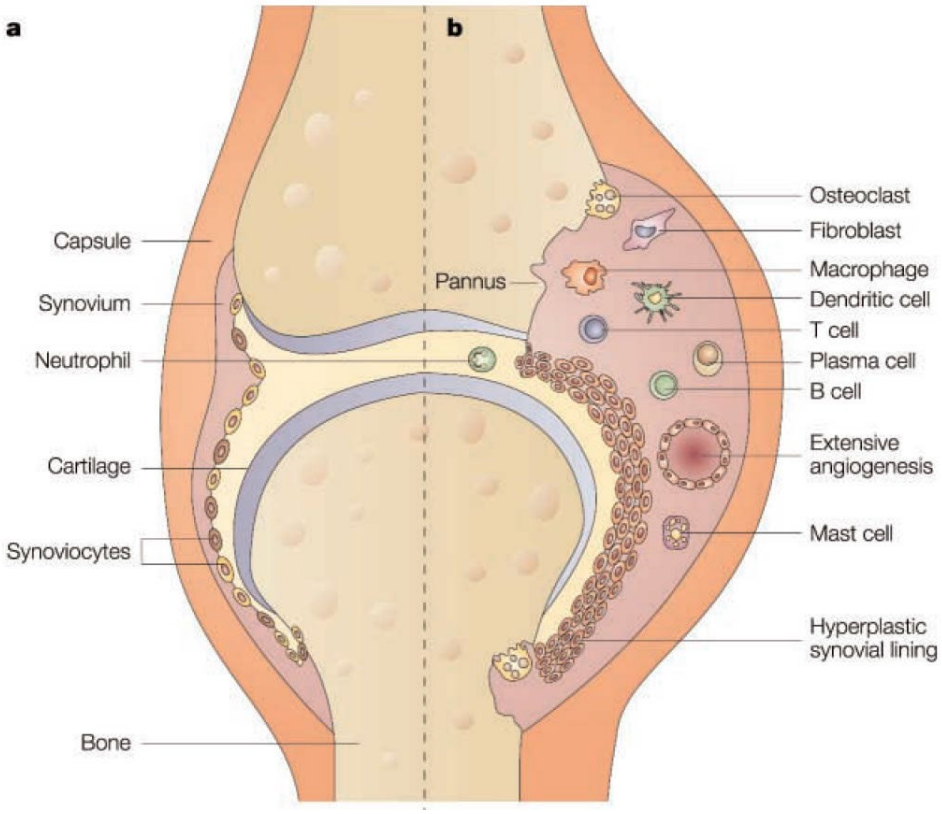

Figure 1: A healthy joint and its RA-induced lesions. *In synovial joints, two adjacent bones are connected, covered by a layer of cartilage, separated by a joint space, and surrounded by a synovial membrane and joint capsule* ***(A)****. As with many other forms of arthritis, RA is initially characterized by an inflammatory response of the synovial membrane, mediated by the trans-endothelial influx and/or local activation of various immune cells, such as T cells, B cells, plasma cells, dendritic cells, macrophages, mast cells, and neutrophilic granulocytes* ***(B)*** *(6).*

Different T helper cell (Th) subpopulations, such as Th1, Th9, Th17, and Th22, are responsible for producing various cytokines, such as tumor necrosis factor-α (TNF-α), interleukin-1β (IL-1β), and IL-22. These cytokines counteract and suppress the effects of anti-inflammatory cytokines (e.g., IL-10, IL-35) that are produced mainly by regulatory T (T_{reg}) and B (B_{reg}) cells. One pivotal aspect of pathogenesis is the activation of resident

macrophages by autoreactive T cells, which leads to further proinflammatory cytokine production (e.g., TNF-α, IL-6, and IL-17) (7, 8). Neutrophilic granulocytes are abundant in the synovial fluid, where they are activated and cause tissue damage by producing lytic enzymes, such as matrix metalloproteases (MMPs), myeloperoxidase (MPO), and reactive oxygen species (ROS). Furthermore, neutrophils release neutrophil extracellular traps (NETs) containing DNA, histones, and lytic enzymes. NETs provide danger signals for other leukocytes and, more importantly, are a source of additional autoantigens, e.g., citrullinated proteins (2, 9). All these inflammatory factors present in the synovium activate resident cells, most importantly fibroblast-like synoviocytes (FLS), which themselves produce various cytokines (e.g., IL-1β, IL-6) and MMPs, thus contributing to further leukocyte recruitment and tissue damage. With the onset of destructive immunologic events, FLS cells become highly invasive and proliferate uncontrollably. Their mobility also increases, and they express β1 integrins on their surfaces that interact with cartilage. FLS can also enter the bloodstream, allowing circulation to carry these cells to healthy joints, where they attach to cartilage and thus cause systemic inflammation of the synovial joints (Figure 2) (10).

As a result, the synovium becomes hypertrophic, leading to joint swelling, stiffness, and pain. This thickened synovium, called pannus, possesses tumor-like properties, as it can invade and destroy the cartilage and the underlying bone. Moreover, hypoxia and various cytokine and chemokine signals induce angiogenesis, resulting in rich vascularization of the pannus and subsequent additional leukocyte infiltration (4).

Osteoclasts play a major role in bone destruction. The differentiation and activation of these cells require both receptor activator of nuclear factor kappa-B ligand (RANKL) and cytokine (mainly TNF-α and IL-6) binding. Several cell types express RANKL on their surface after activation; these include certain T cell and B cell subsets, and fibroblast-like synoviocytes, which are the most prominent in the context of RA. Once the appropriate cytokine environment and RANKL-expressing cells develop in the pannus, strong osteoclastogenesis occurs, leading to high osteoclasts numbers. These cells attach to the bone surface, create an acidic environment, extract minerals from bone, and produce lytic enzymes, such as cathepsin-K, resulting in bone degradation. RANKL and inflammatory cytokines can also enter the circulation, causing systemic bone loss (11).

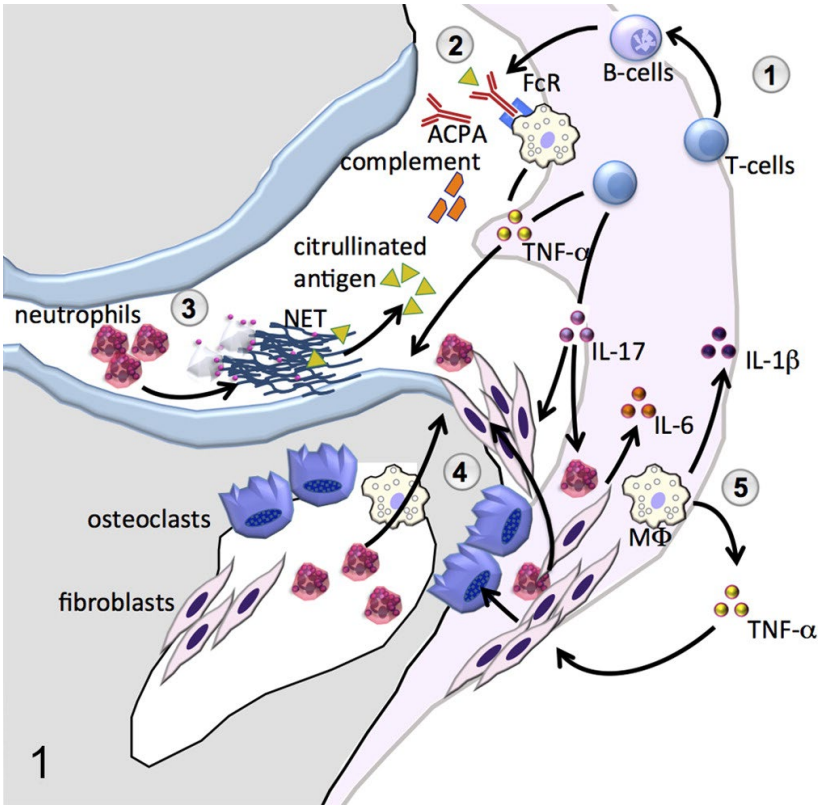

Figure 2: Events that play an important role in the pathomechanism of RA*. Autoreactive T cells are essential components in the induction and maintenance of RA; they assist B cells in activation, and release pro-inflammatory cytokines. ACPAs, other autoreactive antibodies, and complement-mediated effects also play pivotal roles in disease development. Neutrophilic granulocytes contribute to the onset of inflammation by releasing cytotoxic products and immune regulatory mediators. Additionally, they promote autoimmunity by generating NETs that serve as sources of additional autoantigens. The formation of inflammatory pannus leads to bone and cartilage damage. Macrophages infiltrating the synovium (MΦs) play a central role in the pathogenesis of RA. They produce key pro-inflammatory cytokines such as IL-1β and TNF-α. Furthermore, cytokines derived from macrophages and their effects on synovial fibroblasts are essential for osteoclast differentiation and subsequent osteolysis (12).*

1.2. Allergic contact dermatitis

Allergic contact dermatitis (ACD) is an inflammatory skin disease that affects approximately 15% of the world's population. Although it rarely causes severe

conditions, it can substantially reduce the quality of life, and since it is one of the most common occupational health problems, it also has a major socio-economic impact (13). Mechanistically, it is a type IV, so-called delayed-type hypersensitivity (DTH), caused by low molecular weight chemicals, such as urushiol, poison ivy, wool alcohol, rubber mixes, or metal ions, for example, nickel, chromium, cobalt, and gold (14, 15). The pathomechanism of the disease consists of two distinct phases. The first encounter with the allergen initiates the sensitization phase, during which the hapten allergen penetrates the skin barrier and binds to self-proteins, forming a complex antigen. This antigen is recognized and processed mainly by two different types of dendritic cells: Langerhans cells (LCs) in the epidermis or langerin-dermal dendritic cells (DDCs) in the dermis (16, 17). Recently, a third subtype was identified as an important first responder, a γδ T cell receptor (TCR)-expressing T-cell population called dendritic epidermal T cells (DETCs) (18).

After encountering the antigen, these APCs migrate to the skin-draining lymph nodes, where they can present the antigens to naive CD4+ T helper cells (Th) or CD8+ cytotoxic T-cells (Tc), which in turn proliferate and form different subtypes of memory T cells (Th1, Th2, Th17, Tc1, Tc2, Tc17). Repeated exposure to the same allergen initiates the elicitation phase, during which physical symptoms of the condition appear, such as vesicle and blister formation, erythema, and itch. The hapten-protein complex induces the production of chemokines and cytokines from native DDCs, LCs, and keratinocytes, initiating the migration of memory T-cells to the contact site. T cells then produce inflammatory cytokines, including interferon-γ (IFN-γ), IL-1α, IL-6, IL-17, IL-26, TNF-α, and IL-23, and promote further recruitment of cytotoxic T cells and innate immune cells, such as macrophages and neutrophils, to enhance the allergic responses (Figure 3) (19, 20). Keratinocytes primed by IFN-γ and TNF-α express intercellular adhesion molecule-1 (ICAM-I) and major histocompatibility complex II (MHCII), contributing to the recruitment of CD4+ Th1 cells. Although, in the case of DTH, the CD4+ T cells are considered the more critical T cell subset; in ACD, the primary T cell effector functions are attributed to CD8+ T cells. This was described by Gocinski et al., who separately depleted CD8+ and CD4+ T-cells in the CHS mouse model and found that the depletion of Tc cells significantly mitigated, whereas Th cell depletion enhanced allergic reactions (21, 22).

Recently, several studies have demonstrated that innate immune responses play a pivotal role throughout the entire progression of the allergic condition (23-25). Neutrophils are among the first responders to inflammatory signals, recruited by chemokines from the C-X-C family and various cytokines (e.g., IL-1) (26). Studies have shown that neutrophils are essential components in both the sensitization and elicitation phases of the disease (25). Although, it is not yet fully understood how they contribute to the sensitization of the allergen, it is known that during the elicitation phase, they are recruited to the exposure sites by chemokines and cytokines, where they exert their effector responses, such as superoxide and lytic enzyme release. Importantly, neutrophils produce metalloproteinase and granzyme B, which lead to the degradation of the extracellular matrix and the attraction of macrophages to the site of inflammation. Macrophages also contribute to inflammatory responses by producing various cytokines and releasing other mediators. Natural killer cells have been identified as important effector cells of ACD, as they can produce IFN-δ and act similarly to CD8+ T-cells. They are quickly recruited to the site of allergen exposure in response to the chemokine CXCL10 (Figure 3) (27, 28).

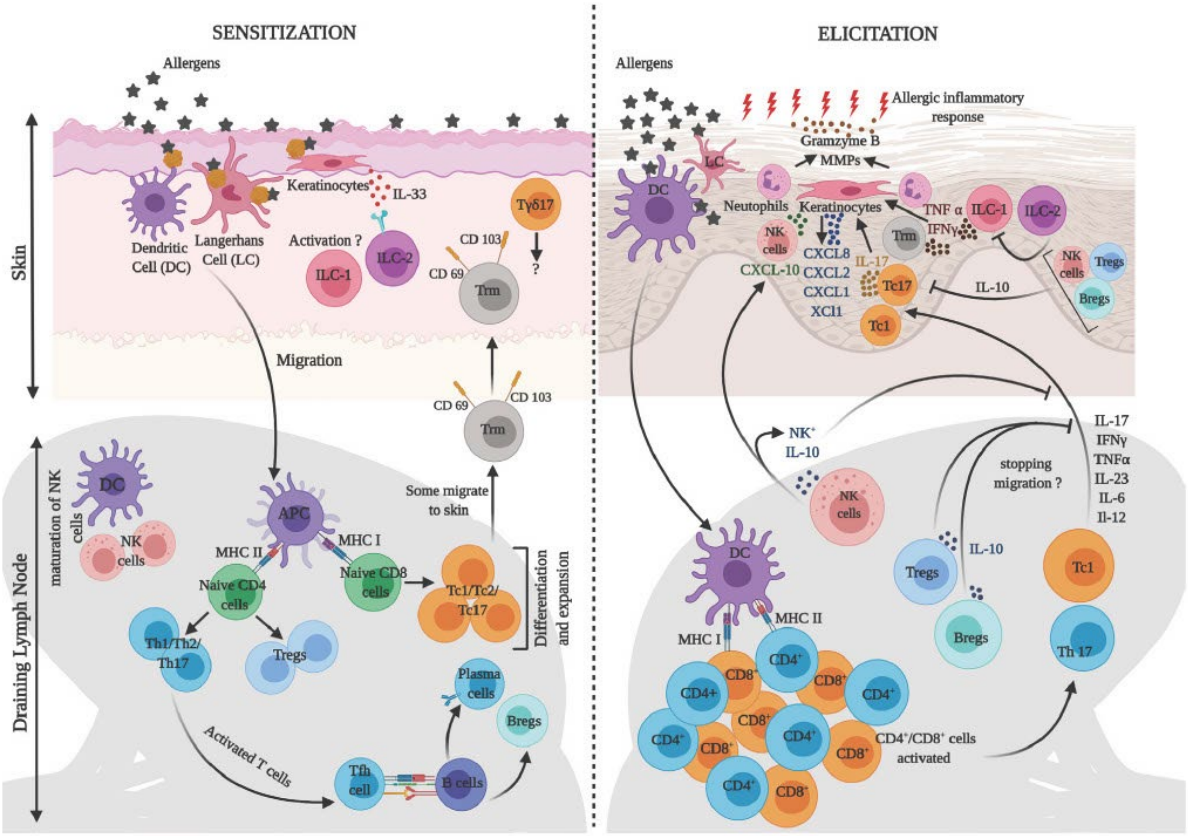

Figure 3: Pathomechanism of allergic contact dermatitis. *In the sensitization phase, dendritic cells (DCs) phagocytose and present the allergens to T cells, activating or transforming them into memory T cells. In the elicitation phase, clonal expansion of the memory T cells takes place. These cells then migrate to the site of exposure and recruit and activate various types of leukocytes, leading to further immunological events and, ultimately, tissue damage (29).*

The complex interplay of all these cell types results in the inflammation of skin tissue and the consequent manifestation of the previously described symptoms.

1.3. Major signaling cascades in inflammation

Several signaling cascades and molecules are crucial in the development of the inflammatory environment in the context of RA and ACD. The p38 mitogen-activated protein kinase (p38MAPK) cascade is involved in numerous cellular processes, such as inflammation, cell proliferation, differentiation, apoptosis, and invasion (30). The pathway can be activated by various cytokines, hormones, or for instance, heat and

osmotic shock (31). In the case of RA, p38MAPK activation was detected in approximately one-third of the synovial cells, including endothelial cells, macrophages, and fibroblasts. This activation plays a role in several immune processes, such as, inflammatory angiogenesis, cytokine (e.g., IL-1, IL-6, and RANKL) and MMP production, expression of adhesion molecules (e.g., E-selectin), and differentiation of osteoclasts (32).

The p38MAPK cascade is primarily initiated by the binding of inflammatory activators (e.g., lipopolysaccharides and cytokines) to their receptors, leading to the recruitment of adapter molecules. Through these adapter molecules and small G proteins (e.g., RAS, RAC, and CDC42), the receptors are connected to the first level of the phosphorylation cascade. After several phosphorylation events, (MAPKKK, MAPKK, then MAPK), different transcription factors, e.g., activating transcription factor-2 (ATF2), are activated, which can initiate the expression of numerous proteins after translocating into the nucleus. One major group of target genes for p38MAPK activation is proinflammatory cytokines such as TNF-α, IL-1, and IL-6. Thus, in inflammatory processes, regulating the expression of these molecules is an important role of p38MAPK (32).

The nuclear factor-κB (NF-κB) signaling pathway is a central and extensively studied component of inflammation. Canonical NF-κB signaling is primarily initiated by TNF-α and IL-1, two important inflammatory cytokines. The binding of these ligands activates the IκB kinase, which phosphorylates IκB. This results in the degradation of IκB, and thus the release of RelA and p50. These two transcription factors of the canonical pathway, then translocate into the nucleus and initiate the transcription of target genes that regulate, e.g., cell survival and innate immune responses. The alternative NF-κB pathway is primarily activated by CD40L, B cell activating factor (BAFF), and RANKL and is independent of IκB. The target genes of the alternative signaling are responsible, e.g., for lymph organ development and B cell activation (33-35). Numerous studies have demonstrated that proinflammatory cytokine production is mediated by the NF-κB pathway in certain inflammatory diseases (36-38). It has also been shown that certain contact allergens activate the NF-κB pathway in the skin aggravating allergic dermatitis (39). Lawrence et al. described that besides the expected role of NF-κB in proinflammatory gene induction during the onset of inflammation, it also activates the expression of anti-inflammatory genes and induces leukocyte apoptosis during the

resolution of inflammation (40). Furthermore, it has been shown that NF-κB inhibits IL-1β processing and secretion in macrophages and neutrophils, while IL-1β induces the release of pro-inflammatory mediators from fibroblast-like synoviocytes via the activation of the NF-κB / ERK / STAT1 pathway (41, 42). These studies demonstrate that activation of the NF-κB pathway is not necessarily pro-inflammatory but can have anti-inflammatory properties as well, highlighting its complex regulatory role in inflammatory diseases (43, 44).

E-cadherin is an integral membrane protein essential for physical cellular interactions. Most importantly, it maintains the barrier function of epithelia through homotypic cell-cell junctions of epithelial cells (45). The cytoplasmic C-terminal end of the protein interacts with catenins and regulates various signaling pathways, including Wnt/β-catenin, PI3K/Akt, RHO GTPase, and NF-κB. In addition, it has been demonstrated that through heterophilic interaction with the inhibitory killer cell lectin-like receptor G1, E-cadherin participates in the regulation of various immune cells such as macrophages, DCs, T cells, and osteoclasts (45).

1.4. Murine models of diseases

Although *in vitro* and *in silico* techniques have significantly advanced in the last decade and are extremely useful tools for many applications, the complex *in vivo* systemic inner environment of a living animal is still the best model of human physiology. Consequently, disease mouse models are essential for understanding human pathophysiologic conditions. Several different mouse models are available for studying RA. Spontaneous models have been developed, such as the tumor necrosis factor TNF-α transgenic and IL-1 receptor antagonist-deficient mice, and induced models have been created, most notably the collagen-induced arthritis (CIA) model and the K/BxN serum transfer arthritis (STA) model. Mouse models have also been developed for the study of dermatitis. NC/Nga mice are susceptible to irradiation and to anaphylactic shock. In these animals, atopic dermatitis spontaneously develops if they are kept in a conventional animal facility, but not if they are in a pathogen free (SPF) environment. However, the 2,4,6-trinitrochlorobenzene (TNCB) induced contact hypersensitivity (CHS) model is much more convenient and accessible (46).

1.4.1. The K/BxN serum transfer arthritis model

The K/BxN model was discovered by crossing T cell receptor (TCR) transgenic KRN mice on a C57BL/6 genetic background with an immunocompromised non-obese diabetic (NOD) mouse strain carrying a mutant MHCII (I-A^{g7}) gene (47). Interestingly, it was found that in the F1 generation offspring of these mice, severe arthritis develops. Later, it was revealed that in these animals, professional antigen-presenting cells (APC) present the ubiquitously expressed glucose-6-phosphate isomerase (G6PI) self-protein on their transgenic MHCII, which is recognized by the KRN TCR of the CD4+ T-cells. This leads to the activation of Th cells, which in turn interact with naïve B-cells via TCR- A^{g7}MHCII and CD40:CD40L connection prompting G6PI-specific autoantibody production, which leads to severe articular inflammation (47-50). Importantly, since the serum of these animals is rich in the G6PI-specific autoantibodies, it has been demonstrated that the transfer of this serum can initiate arthritis in several different mouse strains, including BALB/c, C57BL/6, and DBA/1 mice (Figure 4) (51).

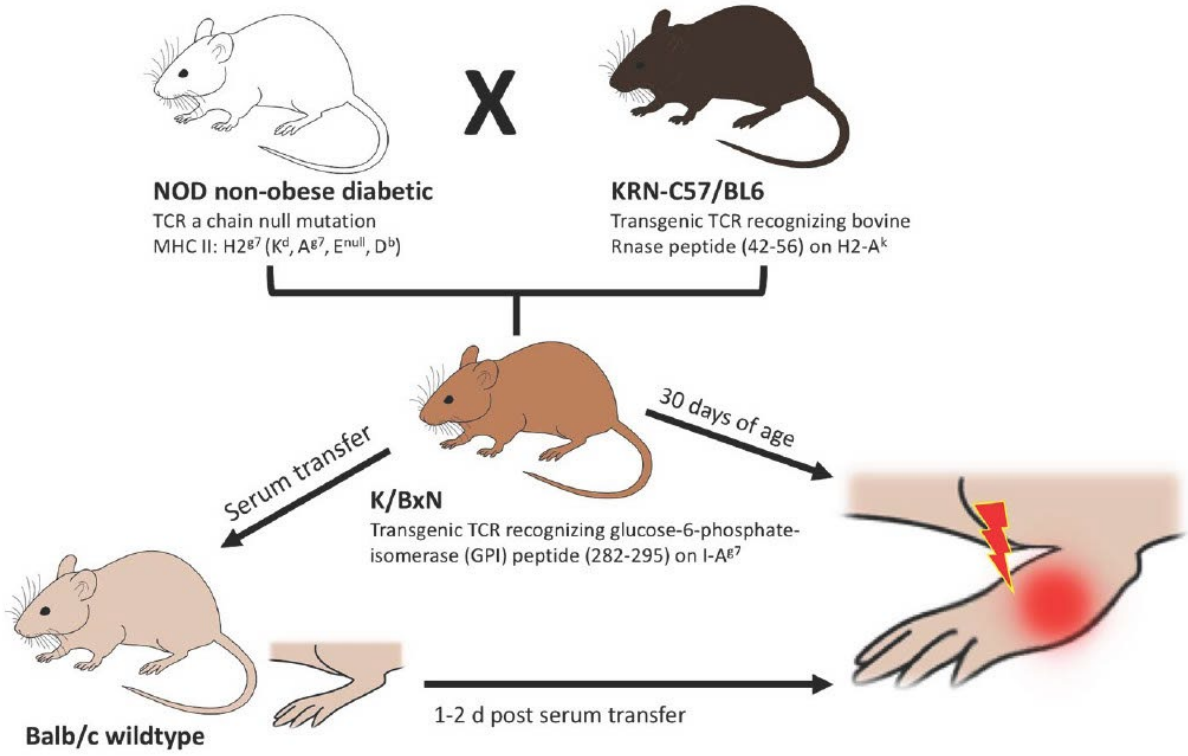

Figure 4: The K/BxN serum transfer arthritis mouse model. *The K/BxN mouse is generated by crossing NOD and KRN-TCR transgenic mice. The F1 offspring develop*

spontaneous arthritis, which can be transferred to various mouse strains via i.p. injection of the arthritogenic blood serum of the K/BxN mice (52).

Investigation of the pathology of the K/BxN mice revealed that the G6PI autoantigen was present on the cartilage surface of normal mice, but it is overexpressed in mice with arthritis, and anti-G6PI antibodies mostly localize to the distal joints (53). It was also shown that these antibodies bind to G6PI here, forming unique immune complexes (ICs) on the cartilage surface (54). Moreover, in the serum of these animals, G6PI and anti-G6PI antibodies form soluble ICs that can activate neutrophils through binding to Fcγ receptors (55, 56). It was suggested that neutrophils then release mediators that increase vascular permeability locally in the small joints, allowing further IC accumulation in the perivascular tissue of the joints. Mast cells may bind these ICs on their FcγRIII receptors and, in turn, release vasoactive mediators of their own, e.g. histamine, that further enhance the permeability of the vessels (55).

It was demonstrated that an important step in disease development is that neutrophils, activated by soluble or cartilage-attached ICs bound to their Fcγ receptors, produce the very potent inflammatory cytokine IL-1β, which in turn induces the release of neutrophil active chemokines, such as CXCL1, CXCL5, and CXCL9, from resident cells in the joint, most notably by synovial fibroblasts (57). Complement fragments, such as complement component 5a (C5a) induce the release of leukotriene B4 (LTB4) from neutrophils, a lipid chemoattractant that can recruit more neutrophils to the synovial cavity in an autocrine manner. LTB4 could also initiate the production of IL-1β. Furthermore, granulocyte colony-stimulating factor (G-CSF), which is likely produced by resident cells in response to IL-1β, drives disease progression, probably by regulating neutrophil numbers (58).

Macrophages are abundant in the synovium of RA patients. Using murine models, it was demonstrated that depletion of macrophages completely protects against RA and that activation of macrophages by IC-FcγR interaction is a crucial step in disease development (59, 60). Furthermore, it was shown that Ly6C- monocytes are recruited to the site of inflammation and differentiate into M1 inflammatory macrophages in the K/BxN STA model. In contrast, tissue-resident macrophages tend to differentiate into the M2, anti-inflammatory phenotype and are important in maintaining joint integrity and resolving inflammation (61). Additionally, granulocyte-macrophage stimulating factor (GM-CSF) is essential for the development of inflammation in this model, since GM-CSF defective

mice and mice treated with GM-CSF blocking antibodies were significantly less susceptible to arthritis, probably due to reduced numbers of circulating monocytes and synovial macrophages (62).

The importance of osteoclasts in autoantibody-induced arthritis was demonstrated using RANKL knockout (KO) mice, which proved to be protected against bone erosion after K/BxN serum treatment (63). Moreover, IL-1β is thought to mediate cartilage destruction, as IL-1R deficient mice were not only completely protected against arthritis but also showed no sign of cartilage destruction after serum treatment (64).

The K/BxN STA model is an extraordinarily useful, robust, and accessible tool for arthritis research, but its limitations must be considered. Histopathological manifestations are similar to RA, with leukocyte invasion, synovitis, hyperplasia, and cartilage and bone destruction (49). However, disease development is significantly faster, with peak inflammation occurring around 6-7 days after serum treatment in the K/BxN model, in contrast to RA, which takes years to manifest. Most importantly, while the induction and pathomechanism of rheumatoid arthritis involve cells and factors of the adaptive immune system, such as different subsets of T cells and B cells, in the K/BxN STA model, exogenous G6PI-specific autoantibodies are administered to the animals, thus bypassing the initiation phase where autoantibodies develop. At the same time, instead of the diverse auto-antibody repertoire responsible for the human disease (e.g., ACPA, RF, anti-collagen-II, but also anti-G6PI), in the mouse model, anti-G6PI is the only type present. Furthermore, while in the K/BxN STA model arthritis induction is solely attributed to autoantibodies, while in RA, although autoantibodies are very important, it is driven by other mechanisms and cells as well, for example, by CD4+ T-cells (65). In summary, this model is beneficial for the investigation of the effector phase but not so much for the initiation phase of RA.

1.4.2. The 2,4,6-trinitrochlorobenzene-induced contact hypersensitivity model

This mouse model is suitable for studying type IV allergic contact dermatitis (ACD) induced by delayed-type hypersensitivity**.** The 2,4,6-trinitrochlorobenzene (TNCB) is a small molecule hapten that, when applied topically to the epidermis, penetrates the skin barrier, binds to the body's proteins and forms protein-hapten complexes, thus acting as a strong allergen. After the first encounter with TNCB (sensitization phase), the protein-hapten complexes in the skin are primarily phagocytosed by dendritic cells and

macrophages, processed, and the antigens are presented to Th1 cells in association with the MHCII molecule, via MHCII-TCR interaction. This results in the development of memory Th1 cells, and upon a second contact with the allergen (elicitation phase), these allergen-specific Th1 cells undergo clonal division, produce cytokines (mainly IFN-γ and IL-12), and recruit macrophages, neutrophils, and cytotoxic T cells to the site of contact. These cells, in turn, can produce their own chemokines and cytokines, leading to further leukocyte recruitment and causing tissue damage by releasing different mediators and by directly destroying cells. Investigation of repeated hapten exposure revealed that this model is also suitable for studying chronic, late-type hypersensitivity. Analyzing the cytokine and cellular composition of the dermal lesions after repeated challenge with TNCB showed that the cytokine profile shifted from a Th1 type more towards a Th2 type (IL-4, IL-5, and IL-10), and parallelly, subepidermal accumulation of CD4+ T-cells is increased. As a result of these changes, elevated titers of antigen-specific IgE were measured in the serum of the animals (46).

Comparing the two murine models, it should be noted that these are two vastly different disease models, not just in their manifestation but also in their pathomechanism. The most prominent difference is that while the K/BxN model is largely dependent on the effector cells of the immune system, in the TNCB-induced hypersensitivity reaction, the inflammatory tissue damage occurs through a more complex process, resulting from the interaction of multiple types of immune cells, involving both the adaptive and the innate arms of immunity.

1.5. ARHGAP25

RAC is a Rho family small GTPase that, in its GTP-bound form, initiates several critical cellular processes. In neutrophilic granulocytes, active RAC is required for the polymerization and the rearrangement of actin filaments. Thus, it is an important regulator of cellular polarization and polarization-dependent mechanisms such as migration, phagocytosis, and adhesion. The slow, endogenous hydrolysis of the bound GTP by RAC results in an inactive, GDP-bound state. Afterward, GDP can dissociate from the small G protein with the help of guanosine exchange factors (GEFs). Since the guanosine nucleotide affinity of small G proteins is very high, and the GTP concentration in the cells is approximately 10 times higher than the GDP concentration, RAC predominantly binds GTP, thus returning to the active state. GTPase activating proteins (GAPs), such as

ARHGAP25, accelerate GTP's slow endogenous hydrolysis and therefore, act as molecular switches that inactivate RAC-dependent cellular processes (66, 67).

ARHGAP25 was initially described as a RAC-specific GTPase-activating protein (GAP) expressed in different leukocytes. The full-length ARHGAP25 protein was cloned and expressed for the first time by our research group and using overexpressing and gene silencing techniques in different cell lines (COS, COSphox, and PLB-985) it was demonstrated, that it is a crucial regulator of different phagocyte effector functions such as phagocytosis and superoxide production (68, 69). Later, our research group purchased an ARHGAP25-deficient mouse strain, and using the mouse cremaster muscle and peritonitis models, described this protein as an essential modulator of transendothelial migration of leukocytes (70). In the framework of a collaboration in the USA, our group also found that ARHGAP25 is required for the normal mobilization of hematopoietic stem cells and progenitor cells (HPSC) from bone marrow in the early stages of leukocyte differentiation (71). In another project, we revealed that the GAP activity of ARHGAP25 is modulated by phosphorylation on three serine residues, and that the phosphorylation pattern contributes to the regulation of different neutrophil effector functions (72). Furthermore, ARHGAP25 was identified as a positive regulator of B cell development and germinal center reactions, as the deletion of this protein resulted in augmented migration toward the cytokine CXCL12 and consequently in increased bone marrow retention of B cells (73). In the last eight years, an increasing number of studies have investigated the role of ARHGAP25 in non-hematopoietic cells, mainly in different types of tumor cells. It was demonstrated that the ARHGAP25 gene is upregulated in alveolar rhabdomyosarcoma cells and increases the invasion capacity of these cells through the RhoE/ROCK/ARHGAP25 signaling pathway (74). On the other hand, in a contradicting study, in three different rhabdomyosarcoma cell lines, ARHGAP25 silencing resulted in the overactivation of the Wnt/β-catenin pathway and increased migration and invasive capacity of these tumor cells, while overexpression of the protein had opposite effects (75, 76). Similarly, it was described that this GAP exerts a tumor-suppressive, anti-metastatic effect in both lung cancer tissues and breast cancer via the inhibition of the Wnt/β-catenin signaling pathway (77-79). In pancreatic adenocarcinoma, ARHGAP25 inhibited glycolysis and, consequently, tumor growth by suppressing the AKT/mTOR pathway (80). Moreover, in colorectal cancer, ARHGAP25 expression was associated

with a favorable prognosis (81). Recently, the role of this GAP was investigated in several non-carcinoma diseases as well. In a human study, a missense mutation in the *ARHGAP25* gene was linked to an increased risk of early-onset skeletal fragility. At the same time, in the central nervous system, astrocyte-derived exosomes attenuated intracerebral hemorrhage-induced blood-brain barrier disruption through silencing ARHGAP25 via a micro-RNA (82, 83).

It should be mentioned that despite its significantly lower expression, ARHGAP25 is an important regulator of cells of non-hematopoietic origin, suggesting even more relevance in the immune compartment.

All the aforementioned research findings collectively demonstrate that ARHGAP25 plays a critical role as a modulatory protein in both physiological and pathological processes, indicating its potential significance as a therapeutic target for various conditions.

Although ARHGAP25 clearly acts as a GAP on RAC small G protein, and in recent years it was connected to several signaling pathways (Wnt/β-catenin, AKT/mTOR) in different tumor cell lines, it is still not unquestionably clear what molecular mechanisms are responsible for the various effects of this protein. Therefore, our research group recently aimed to find new protein partners and to reveal the interactome of ARHGAP25 in neutrophils. In this work, we managed to find 76 candidates of protein interaction, such as small GTPases other than RAC (RHOG, ARF4, and RAB27A), several Fc receptor-related kinases, phosphatases, and three of the 14-3-3 members, as well as signaling molecules connected to interleukins (84).

Based on these data, we suspect that ARHGAP25 asserts its regulatory effect through the interplay between numerous different proteins in several different cell types.

1.6. Current therapeutic strategies

There are several traditional approaches to the treatment of RA. As a first line of defense, glucocorticoids (GC) and nonsteroidal anti-inflammatory drugs (NSAIDs) are typically used, as they quickly alleviate pain and reduce inflammation, but have a short-lasting effect. These drugs are effective in the early weeks after the onset of clinical symptoms, thus they are mostly used as a transitional treatment before the slow-acting disease-modifying antirheumatic drugs (DMARDs) take effect (85). NSAIDs are a group of cyclooxygenase inhibitors, which decrease the level of prostaglandins. However, their prolonged usage can lead to severe side effects, affecting mostly the gastrointestinal

system and the kidneys (86, 87). NSAIDs that selectively block cyclooxygenase-2 were reported to have a better gastrointestinal side effect profile but may increase the risk of cardiovascular complications (88, 89). Glucocorticoids act through two distinct mechanisms. On one hand, as steroid hormones, they can bind to intracellular receptors and suppress the transcription of different genes, coding proinflammatory cytokines such as IL-1β, IL-2, IL-3, IL-6, TNF-α, IFN-γ, and IL-17 (90). On the other hand, GCs can act on plasma membrane receptors on certain monocytes, B cells, and T cells, thus also having an immediate effect (91).

Several DMRADs are used in clinical practice. These molecules have diverse structures and beneficial effects. The most commonly used one is methotrexate, which can suppress leukocyte proliferation, reduce the accumulation of toxic compounds, decrease the intracellular level of glutathione, and increase the extracellular level of adenosine. All these mechanisms together help to alleviate inflammation and diminish tissue damage (92-94). Sulfasalazine decreases immunoglobulin levels, inhibits neutrophil functions, and blocks NF-κB (95). By unknown mechanisms, hydroxychloroquine seems to impair deoxyribonucleotide metabolism, interfere with the antigen presentation, and stabilize lysosomal membranes (96, 97). As an immunomodulatory agent, leflunomide interferes with the synthesis of pyrimidines, which are crucial for lymphocyte activation (98). These drugs can be effective tools but predominantly soothe the symptoms of RA without targeting the root causes of the disease. On the other hand, they have broad targets and are not specific, thus they can have diverse side effects.

For these reasons, biological treatments with higher target specificity have gained significant attention. One class of TNF-α inhibitors has been developed, including monoclonal antibodies (mAb), mAb fragments, and fusion proteins. The first one was infliximab, which is a chimeric murine-human mAb (99). Adalimumab is a fully human, recombinant mAb, thus it has lower immunogenicity (100). Etanercept is a fusion protein, containing the human TNF receptor and the Fc portion of human IgG1, providing very high target specificity (101). These molecules not only block TNF-α action, but through their Fc portion can trigger effector immune functions on TNF-α target cells. This way, they can initiate phagocytosis, antigen-dependent cellular cytotoxicity, and complement-mediated lysis. Despite their higher target specificity, TNF-α inhibitors are associated

with several side effects, such as susceptibility to infections, nausea, headache, and higher risk of malignancies (102, 103).

Another class of biologics is co-stimulation blockers (e.g. Abatacept) which inhibit T cell activation (104). Other targets for biological treatment include the CD20 molecule on B cells with rituximab (105), and the enzyme Janus kinase (JAK, e.g. tofacitinib), which is a prominent component in the signal transduction of most proinflammatory cytokines (106).

These biologics are often used in combination with traditional drugs, mostly with methotrexate, which increase their efficacy (107).

Finally, it should be mentioned that in recent years, cell-based therapies have emerged as promising candidates for patients who do not respond well to conventional and biological treatments (108). Therapies with mesenchymal stem cells, hematopoietic stem cells, embryonic stem cells, and human amniotic membrane cells show good results. Non-stem cell-based therapies, using regulatory T cells and chimeric antigen receptor T cells, are also being developed (109).

The literature on ACD therapy is less extensive. This is probably due to the fact that when the allergen is identified, avoidance of contact is the most effective and simple way to prevent symptoms. However, avoidance is not always possible when the allergen itself is unidentified or, for example when the patient is reacting to a necessary medical device, or if contact is integral to the patient's occupation. In these cases, pharmaceutical therapy is required for the remedy of the symptoms of ACD (110).

Since both RA and ACD are inflammatory diseases, certain treatment methods that target the resolution of inflammation overlap. In the case of ACD, if the symptoms are not yet extensive, topical therapy is implemented. In cases when the symptoms cannot be controlled by topical treatment, systemic therapy is required. Corticosteroids can be used in ACD both locally and in severe cases systemically, but prolonged administration causes diverse side effects (111). Calcineurin inhibitors such as tacrolimus or cyclosporine suppress T cell activation and have a favorable side effect profile even if used chronically (112). JAK inhibitors are promising candidates for topical and systemic eczema, and possibly for ACD treatment (113, 114).

Oral administration of methotrexate can also be effective in treating ACD since it remedies inflammation through several different mechanisms described previously (115).

Although few studies investigate biologics in ACD therapy, monoclonal antibodies targeting inflammatory cytokines show promising results, with few side effects. In a clinical study, the TNF-α inhibitor infliximab proved to be effective (116). The injectable IL-4 receptor antagonist dupilumab inhibits both IL-4 and IL-13 action by binding to their receptors. Several studies describe successful treatment with this drug that was well tolerated by patients, probably due to its high target specificity (117, 118).

In recent years, novel therapeutic strategies have been developed for the treatment of both RA and ACD. With the use of biologics, better target specificity was achieved, leading to an improved side effect profile. However, the efficacy of the different drugs shows significant variability in the population, and side effects can still cause serious complications. Furthermore, the manufacture of biologics is quite a complex and, thus, expensive process.

For these reasons, identifying novel drug targets and developing new therapeutic strategies are still very much needed.

2. OBJECTIVES

ARHGAP25 is a crucial regulator of phagocytes and is also highly expressed in other leukocytes, such as lymphocytes. Furthermore, the effect of this protein on tumor invasion and metastasis underscores its relevance in pathophysiological conditions. However, there is currently no data on the role of ARHGAP25 in inflammatory diseases, where pathological conditions arise from the interplay between different types of leukocytes and other cells.

Therefore, during my PhD studies, I aimed to investigate the role of this protein in mouse models of two mechanistically different diseases: The K/BxN serum transfer arthritis model and the TNCB-induced allergic contact hypersensitivity model. Our main questions were the following:

1. Does ARHGAP25 influence the symptoms of autoantibody-induced arthritis and allergic contact hypersensitivity?

2. If it does, which immune cells are responsible for these changes? What other cells besides leukocytes, if any, are involved?

3. Does ARHGAP25 alter the cytokine composition of inflamed tissues? If so, which cytokines might be significant?

3. MATERIALS AND METHODS

3.1. Experimental animals

For our experiments, age-matched male mice were used. Wild-type and *Arhgap25* knock-out mice on a C57BL/6 background were kept and bred individually in sterile ventilated cages (Tecniplast, Buguggiate, Italy) in a specific pathogen-free (SPF) animal facility of Semmelweis University. All experiments were in line with the EU Directive 2010/63/EU for animal experiments act and were approved by the Animal Experimentation Review Board of Semmelweis University and the Government Office for Pest County, Hungary (Ethical approval numbers: PE/EA/1967-7/2017, BA/73/00070-2/2020.).

Arhgap25$^{-/-}$ bone marrow chimeric mice were generated by lethal irradiation of wild-type (WT) recipient animals carrying the CD45.1 allele on a C57BL/6 genetic background with 11 Gy from a 137Cs source using a GSM D1 irradiator as described previously (119). This was followed by the injection of unfractionated bone marrow cells isolated from femurs and tibias of *Arhgap25*$^{-/-}$ mice (carrying the CD45.2 allele) into the retroorbital plexus of recipient animals. In the case of reverse bone marrow chimeras, *Arhgap25*$^{-/-}$ mice were irradiated, and donor cells from WT mice carrying the CD45.1 allele were used for injection.

After 4 weeks, to verify the repopulation of the hematopoietic compartment by donor-derived cells, peripheral blood samples were collected and labeled for Ly6G and CD45.1 or CD45.2. The samples were analyzed with flow cytometry (CytoFLEX, Beckman Coulter). The ratio of donor-derived cells among neutrophils was quantified. Only mice, in which over 95% of the cells originated from the donor animals, were used for experiments.

3.2. Disease induction

3.2.1. Induction of autoimmune arthritis

T cell receptor transgenic KRN$^{+/-}$ male mice were crossed with Ag7 MHC II$^{+/+}$ NOD/Lt female mice, both on a C57BL/6 genetic background, and the arthritic (K/BxN) serum of the F1 offspring, as well as control (BxN) serum from their transgene-negative littermates, was collected in the laboratory of Professor Attila Mócsai. To induce autoimmune arthritis in our experiments, WT, *Arhgap25*$^{-/-}$, or bone marrow chimeric mice were injected i.p. with 150 µl pooled K/BxN or BxN serum diluted in sterile phosphate-

buffered saline (PBS). Before treatment, and after that, every 24 hours, for 8 days, the severity of arthritis was assessed by an observer blinded to the experiment. First, clinical scoring of both hind limbs was performed on a 0-10 scale based on the visible signs of inflammation (swelling, redness, and appendage disfigurement), and after, ankle thickness was measured with a spring-loaded caliper (Kroeplin) (120, 121).

3.2.2. Induction of contact hypersensitivity

The induction of contact hypersensitivity was carried out by topical treatment of the shaved skin on the abdomen of the experimental animals with 3% (m/V) TNCB dissolved in acetone, which triggers the sensitization phase. Control mice received acetone treatment only. Therefore, no sensitization is induced in them at this point. Five days later, under isoflurane anesthesia, ear thickness was measured using a microcaliper (by a blinded observer). Afterward, the ears were coated with 1% (m/V) TNCB in the case of both previously TNCB-treated, and control animals. In the formerly TNCB-treated group, this second exposure to the allergen triggers the elicitation phase. In the control group, this is the first contact with TNCB; thus, the sensitization phase is initiated in them. After 24 hours, ear thickness was measured under anesthesia again, then the mice were sacrificed, and the ears were removed for further analysis.

3.3. Detection of hind paw volume by plethysmometry

Hind paw volume measurement of K/BxN and BxN serum-treated animals was performed before arthritis induction and each day thereafter, every 24 hours for 8 days, using a plethysmometer (Ugile Basile). The volume measurement is performed by immersing the hind paw into a water-filled glass tube. The instrument uses a force transducer, which measures the displaced fluid volume, and according to this, calculates the paw volume expressed in cubic centimeters (cm^3). The mean volumes of both hind paws were calculated and used for data analysis (121).

3.4. Joint function measurement

Horizontal grid test was used to measure the grasping ability of mice 3, 6, and 8 days after arthritic or control serum administration. The animals were placed on a horizontal wire grid, which was flipped over slowly. When the grid was upside-down, the time after the mice fell from the grid was measured (for 20 seconds maximum). On each day, three

separate measurements were carried out with each mouse, and the average was used for evaluation with Kaplan-Meier survival analysis (120). To correct for the individual differences in grasping ability between the mice, all the mice were trained on the wire grid on three different days, three times each day, before serum treatment.

3.5. Assessment of touch sensitivity

Measurement of the mechanonociceptive thresholds of the hind paws of mice was performed with a dynamic plantar aesthesiometer (DPA, Ugo Basile), before and 3, 6, and 8 days after serum treatment (122). The animals were individually placed into plexiglass boxes with wire grid bottoms where they could move freely. Hind paws were touched with a metal filament from below with gradually increasing force (up to 10 g with 4 s latency) until the avoidance movement happened. The measurement was performed three times on both hind paws, and the mean was calculated to obtain the mechanonociceptive threshold, which was expressed in grams (g).

3.6. Histology

In the case of the K/BxN experiments, animals were anesthetized terminally 8 days after serum treatment. Ankles were removed, fixed using 4% buffered formaldehyde, decalcified, dehydrated, and embedded in paraffin. Afterwards, 5 µm thick sections were prepared, and hematoxylin and eosin (HE) or Safranin O were used for staining. Images were captured, and sections were evaluated by a trained observer blinded to the experimental setup. Synovial hyperplasia (represented by the fibroblast abundance), collagen deposition, and cartilage destruction were inspected and scored on a 0-3 scale (122).

In the case of contact hypersensitivity measurements, 24 hours after TNCB treatment of the ears, mice were sacrificed, the ears were harvested, and hematoxylin-eosin staining was performed similarly as described above, with the difference that in the case of ear tissues, decalcification was not necessary. Afterward, representative images of the sections were captured using a Nikon microscope.

3.7. In vivo luminescence measurement of myeloperoxidase activity

Neutrophil-derived MPO activity imaging was carried out in vivo using the IVIS Lumina III In Vivo Imaging System (PerkinElmer) (123, 124). The animals were anesthetized

with ketamine (Calypsol, Gedeon Richter Plc.; 120 mg/kg i.p.) and xylazine (Sedaxylan, Eurovet Animal Health B.V.; 6 mg/kg i.p.), and to avoid signal distortion, the hair was completely removed from the hind limbs, one day before arthritis induction (day -1). MPO activity was assessed at 24 and 48 h and on day 7 of the experiments. Prior to the measurements, the anesthetized mice were injected intraperitoneally with Luminol sodium salt (Gold Biotechnology) dissolved in 1x PBS (30 mg/mL, 150 mg/kg). Bioluminescence intensity was measured 10 min after luminol administration (120 s acquisition, Binning=8, F/Stop=1). During the evaluation of the captured images, identical regions of interest (ROIs) were selected on the hind paws of the animals, and luminescence was expressed as total radiance (total photon flux/s) within the ROIs.

3.8. In vitro superoxide production measurement of neutrophils

To isolate polymorphonuclear neutrophils (PMN), mice were sacrificed, the femurs and tibias were excised and flushed with Hank's balanced salt solution (HBSS, HyClone), and the obtained bone marrow was filtered using a cell strainer with 70 μm pore size (Greiner) and centrifuged. Afterward, erythrocytes in the cell pellet were hemolyzed using hypotonic NaCl (Biolab) solution (lysis was stopped with the addition of hypertonic NaCl, resulting in an isotonic solution). Following another centrifugation step, neutrophils were isolated Percoll gradient centrifugation (PMN will sediment onto the bottom of the Falcon tubes), and cell numbers were determined by counting in a Bürker chamber after Türk staining.

Afterward, three different stimuli were used to induce the superoxide production of the obtained neutrophils. i., Immune complex surface was created on 96-well microtiter plates (Nunc maxisorp) by first coating the wells with 20 μg/mL human serum albumin (HSA, Sigma Aldrich) in bicarbonate-containing buffer (35 mM NaHCO3 and 15 mM Na2CO3). Wells were blocked with 10% (w/v) fetal bovine serum (FBS, Capricorn Scientific) diluted in HBSS, and finally, HSA-specific antibody (Sigma-Aldrich) was added at a 1:200 dilution in HBSS containing 10% (w/v) FBS. Between each step, wells were washed with HBSS. ii., To generate an integrin activating surface, wells were coated with fibrinogen (Calbiochem) in 150 μg/mL final concentration, diluted in HBSS, and after washing, 100 ng/mL mouse TNF-α (Sigma-Aldrich) was added. iii. Phorbol 12-myristate 13-acetate (PMA, Sigma-Aldrich) was used at a concentration of 100 nM. In each superoxide experiment, $4x10^5$ neutrophils in HBSS containing 100 μM

ferricytochrome c (Sigma-Aldrich) were pipetted in each well. The neutrophils' basal superoxide production was also measured without stimulus. Then, optical density (OD at 550 and 540 nm wavelengths) was measured for one hour with an ELISA reader (ThermoFisher Scientific). For evaluation, the amount of superoxide produced by 10^6 cells was calculated after subtraction of the basal values.

3.9. Leukocyte infiltration measurements

In the case of the autoimmune arthritis experiments, 5 days after serum injection, mice were sacrificed, and using a syringe, ankle joints were flushed out with ice-cold PBS containing 20 mM N'-2-hydroxyethylpiperazine-N'-2-ethanesulfonic acid (HEPES, Sigma-Aldrich) and 10 mM ethylenediaminetetraacetic acid (EDTA, Sigma-Aldrich). Next, samples were centrifuged, and the supernatants were saved. The sedimented cells were used to perform flow cytometry. For this, cells were stained with PerCP-Cy5.5-conjugated anti-Ly6G and Phycoerythrin-conjugated F4/80 specific antibodies (ThermoFisher Scientific) diluted in PBS containing 5% FBS. Then, samples were washed twice with PBS, resuspended in FACS lysis buffer (BD bioscience) and finally, 50 µL of each sample was measured with a Cytoflex cytometer (Beckman Coulter) in each sample.

In the case of the allergic contact hypersensitivity model, harvested ears were cut into small pieces, and the connective tissue was digested using 200 µg/mL Liberase enzyme cocktail (Roche) in Hank's Balanced Salt Solution (HBSS, Cytia) supplemented with 200 mM HEPES (Sigma-Aldrich). Afterward, the samples were filtered through a cell strainer (Sigma-Aldrich) centrifuged, and supernatants were saved for cytokine measurements. Then, sedimented cells were resuspended and divided into two equal parts. In one part, leukocytes (with CD45-FITC), myeloid cells (with CD11b-eFluor450), neutrophil granulocytes (with Ly6G-PerCP-Cy5.5), and macrophages (with F4/80-PE) were labelled with specific antibodies. In the other, leukocytes (CD45-FITC), T cells (CD3-eFluor450), helper T-cells (CD4-PerCP-Cy5.5), and cytotoxic T cells (CD8-PE) were stained (all antibodies were purchased from ThermoFisher Scientific). After two washing steps, 50 µL of each sample was measured with a Cytoflex cytometer (Beckman Coulter), and a multi-step gating strategy was used to determine the number of different leukocytes in the ears.

3.10. Cytokine measurements

The cell-free supernatants of the flushed-out ankle and digested ear samples were used for the cytokine measurements. The concentrations of IL-1β and macrophage inflammatory protein-2 (MIP-2) were measured in both disease models using enzyme-linked immunosorbent assay (ELISA) kits (R&D Systems), using the protocols provided by the company. In digested ear supernatants, the cytokine profile was assessed from pooled samples (from 9 mice per group) using a Mouse Cytokine Array kit (R&D Systems), following the manufacturer's instructions.

3.11. Analysis of the possibly affected signaling pathways

Five days after K/BxN or BxN serum treatment, ankles were excised, snap-frozen and ground up in liquid nitrogen, and then treated with lysing buffer (30 mM Na- HEPES, 100 mM NaCl, 1% [w/v] Triton- X-100, 20 mM NaF, 1 mM Na-EGTA, 1 mM Na-EDTA, 100 mM benzamidine, % [w/v] aprotinine, 1% [w/v] protease inhibitor cocktail, 1% [w/v] phosphatase inhibitor cocktail, and 1% [w/v] phenylmethylsulfonyl fluoride; pH 7.5) on ice for 10 minutes. After the total protein concentration of the lysates was determined according to Bradford, 40 µL of each sample was run on 4-15% polyacrylamide gradient gels (Bio-Rad). The separated proteins were blotted to nitrocellulose membranes (Bio-Rad). After blocking with EveryBlot Blocking Buffer (Bio-Rad), membranes were labeled overnight at 4°C with the indicated phosphoprotein-specific primary antibodies (Table 1). Then, horseradish peroxidase-conjugated rabbit IgG-specific secondary antibody (GE Healthcare) was used to detect bound primary antibodies. After the development to x-ray films (Fujifilm), the antibodies from the membranes of phosphorylated ERK and MAPK were stripped with 2% Sodium dodecyl sulfate (SDS, Sigma-Aldrich) and 0.7% 2-mercaptoethanol (Serva) in PBS at 55°C for 20 minutes and labeled with the antibodies specific to the appropriate total proteins (Table 1). Following another stripping of bound antibodies, membranes were decorated with anti-GAPDH antibody as a loading control (Cell Signaling antibody, 1:5000). Membranes labeled with I-kB-specific antibodies were stripped only once to detect GAPDH. The E-cadherin and β-catenin labeled membranes were not stripped since their molecular weight does not overlap with GAPDH, and phosphorylated forms were not detected. Densitometry was performed using ImageJ software (ver. 1.53o). For data normalization, GAPDH was used

in the case of total protein signals and the corresponding total protein in the case of phosphoprotein signals.

3.12. Determination of ARHGAP25 protein levels in fibroblast-like synoviocytes

Arthritis was induced as described previously; mice were sacrificed after seven days, and all four ankles were harvested. The skin was removed, and sterile 70% ethanol and then HBSS were used to wash the ankles. Afterward, the joints were fragmented and incubated in HBSS containing 20 mM HEPES and 80 mg Liberase enzyme cocktail (Roche) at 37°C for one hour with 1400 RPM shaking. Following the filtration of the samples on a 70 μm pore size strainer (Greiner), they were centrifuged, the pellets were washed twice with HEPES containing HBSS and finally resuspended in 10 mL Dulbecco's modified Eagle medium with GlutaMAX I (Lonza) supplemented with 10% (w/v) FBS, 50 units/mL penicillin, and 50 mg/mL streptomycin. The cells obtained this way were cultured in a 5% humidified CO_2 incubator at 37°C for a minimum of one week on tissue culture Petri dishes (Orange Scientific). To determine the ARHGAP25 content of synovial fibroblasts, cells were collected using trypsin-EDTA, then lysed and blotted as previously described. Finally, membranes were incubated with anti-ARHGAP25 and anti-GAPDH primary antibodies, then with HRPO (horseradish peroxidase) conjugated, rabbit IgG-specific secondary antibody (Table 1).

Table 1: Antibodies used for Western blot analysis.

Specificity	Dilution	Manufacturer	Catalog number	RRID
Total-p44/42 ERK 1/2	1:1000	Cell Signaling	4695S	AB_390779
Total-p38 MAPK	1:1000	Cell Signaling	9212S	AB_330713
Total-NF-κB p65	1:1000	Cell Signaling	8242S	AB_10859369
Total-E-cadherin	1:1000	Cell Signaling	#3195	AB_2291471
Total-I-κB	1:1000	Cell Signaling	4812S	AB_10694416
Total-β-catenin	1:500	Cell Signaling	#8480	AB_11127855
Phospho- p44/42 ERK 1/2	1:1000	Cell Signaling	4370S	AB_2315112
Phospho-p38 MAPK	1:1000	Cell Signaling	4511S	AB_2139682
GAPDH	1:5000	Cell Signaling	14C10	AB_561053
ARHGAP25	1:5000	ImmunoGenes	-	-

rabbit IgG (secondary)	1:5000	GE Healthcare	RPN4301	AB_2650489

3.13. In vitro migration assay

Wild type and *Arhgap25*$^{-/-}$ animals were sacrificed, bone marrow was flushed from their femur and tibia, and PMN were isolated as previously described (see section 4.9). Afterward, wells of 24-well tissue culture plates and transwell inserts (3 µm pore size; Corning) were blocked with 10% FBS. Then, cell-free and pooled (9 samples per experimental group) supernatants of the ear lysates of the different treatment groups of WT and KO animals were diluted 2-fold with HBSS for the stimulus. Wells were filled with 1 mL of these supernatants, and inserts were loaded with $2x10^5$ neutrophils in a 200 µL volume. After a one-hour, 37℃ incubation step, plates were centrifuged, inserts were removed, and transmigrated PMN numbers were determined using an acid phosphatase assay (125, 126).

3.14. Separation of mouse ear epidermis

Harvested ears were washed with distilled water and disinfected for 5 minutes in 70% ethanol. Then, the ears were washed three times and digested in 5 mg/mL Dispase II (Sigma Aldrich) dissolved in DMEM culture medium (Lonza) for 24 hours at 4℃. Afterward, epidermis was peeled off from the ears, cleaned from the remaining connective tissue, washed, then frozen and grinded up in liquid nitrogen for quantitative reverse transcription polymerase chain reaction (RT-qPCR) and western blot (WB) experiments.

3.15. Collection of human skin samples

After informed consent, skin tissue samples were harvested from patients diagnosed with ACD. Symptomatic and asymptomatic sampling areas were selected and biopsied by a trained dermatologist. Before sampling, the selected skin area was disinfected and anesthetized with lidocaine infiltration. Skin samples were excised using a 5mm punch biopsy instrument. After hemostasis, the defect was primarily closed with a simple knotted suture. Tissue samples were placed on dry ice in sterile Eppendorf tubes immediately after excision. Human sampling and experiments were approved by the Committee of Science and Research Ethics of the Medical Research Council (ETT

TUKEB) and by the Department of Health Administration of the National Public Health Center of Hungary (Ethical approval number: IV/1707-6/2020/EKU).

3.16. Gene expression analysis

Ground human skin and murine ear samples were lysed using TRI Reagent™ (Invitrogen) and stored at -80°C until RNA preparation. Total RNA was extracted following the protocol provided by the manufacturer. cDNA was synthesized using iScript™ gDNA Clear cDNA Synthesis Kit (Bio-Rad) according to the manufacturer's instructions. A LightCycler® 480 system (Roche) with TaqMan hydrolysis probes (see Table 1) was used to measure relative expression levels of murine *Arhgap25* and human ARHGAP25. The reference genes were mouse ribosomal protein lateral stalk subunit p0 (Rplp0) and human RPLP0, respectively. Data analysis was performed using the second derivative maximum method, LightCycler® Relative Quantification Software (version 1.5.0.39, Roche).

3.17. T cell numbers and activity measurements of lymph node-derived cells

The shaved abdominal skin of animals was painted with either 3% (m/V) TNCB or vehicle, five days later mice were sacrificed, and the inguinal and axillary lymph nodes were excised. The lymph nodes were homogenized in PBS and filtered using cell strainers with 70 μm pore size. Using the pooled samples of the four lymph nodes of each animal, total cell numbers were counted in a Bürker chamber, then parts of the samples were labelled for 1 hour at 4℃ with fluorophore-conjugated antibodies: CD3-eF450, CD4-PerCP-Cy5.5, CD8-PE, CD69-APC, CD25-FITC (ThermoFisher Scientific, concentration was added according to the instructions of the manufacturer). After three washing steps with PBS, samples were fixed using fax lyzing buffer (Sigma Aldrich) and measured by flow cytometry. Using a multi-step gating strategy, the number of T helper cells ($CD3^+CD4^+$) and cytotoxic T cells ($CD3^+CD8^+$) and the ratios of activated T cells ($CD25^+$ or $CD69^+$ cells) within the two T cell types were determined.

3.18. Transfer of lymph node cells into recipient animals

In each case, five million cells of the remaining lymph node-derived samples (obtained as described above) were centrifuged, resuspended in alpha-MEM medium (Capricorn Scientific), and injected into the retroorbital plexus of resting recipient mice. The three experimental groups were the following: WT lymph node cell receiving WT recipient

mice (WT→WT), WT lymph node cell receiving *Arhgap25*$^{-/-}$ recipient mice (WT→*Arhgap25*$^{-/-}$), and *Arhgap25*$^{-/-}$ lymph node cell receiving WT recipient mice (*Arhgap25*$^{-/-}$→WT). In each case, lymph node cells from mice sensitized with TNCB were used. One hour after the cell transfer, we measured the ear thickness of the recipient animals and treated the ears with 1% (m/V) TNCB. After Twenty-four hours, ear thickness was measured again, and in each case, the increase of ear thickness was calculated.

3.19. Statistical analysis

Data was analyzed and plotted using GraphPad Prism 10.0.1 software. In the case of horizontal grid test, comparison of experimental groups was performed by Kaplan-Meier survival analysis, followed by log-rank test. Analysis of histology was performed with the Mann-Whitney test. Two-way ANOVA with Tukey's multiple comparison tests was used in all other cases. All p values $<.05$ were considered statistically significant.

4. RESULTS

4.1. In ARHGAP25-deficient animals, arthritic joint inflammation is significantly mitigated

First, the K/BxN serum transfer arthritis mouse model was used to investigate the possible regulatory role of ARHGAP25 in inflammatory processes in vivo. Each day after treatment with the serum, hind paw morphology was assessed using a semiquantitative scoring system, based on the visible signs of inflammation, e.g., swelling, redness, and appendage disfigurement. In WT animals, arthritogenic (K/BxN) serum treatment resulted in intense visible inflammation, whereas control (BxN) serum did not induce any inflammation (Figure 5A). In contrast, in ARHGAP25-deficient (KO) animals, only a moderate change in hind paw morphology was observable compared to control serum-treated KO mice (Figure 5A). Interestingly, we found that the clinical severity was reduced by approximately 50% in the KO animals compared to WT after arthritogenic serum treatment (Figure 5B). This result was confirmed by the more objective ankle thickness (measured with a caliper) and paw edema (measured by plethysmometry) measurements, meaning that in both cases, we observed a similar, significant reduction in the KO, arthritic mice compared to the WT arthritic ones (Figure 5C, D).

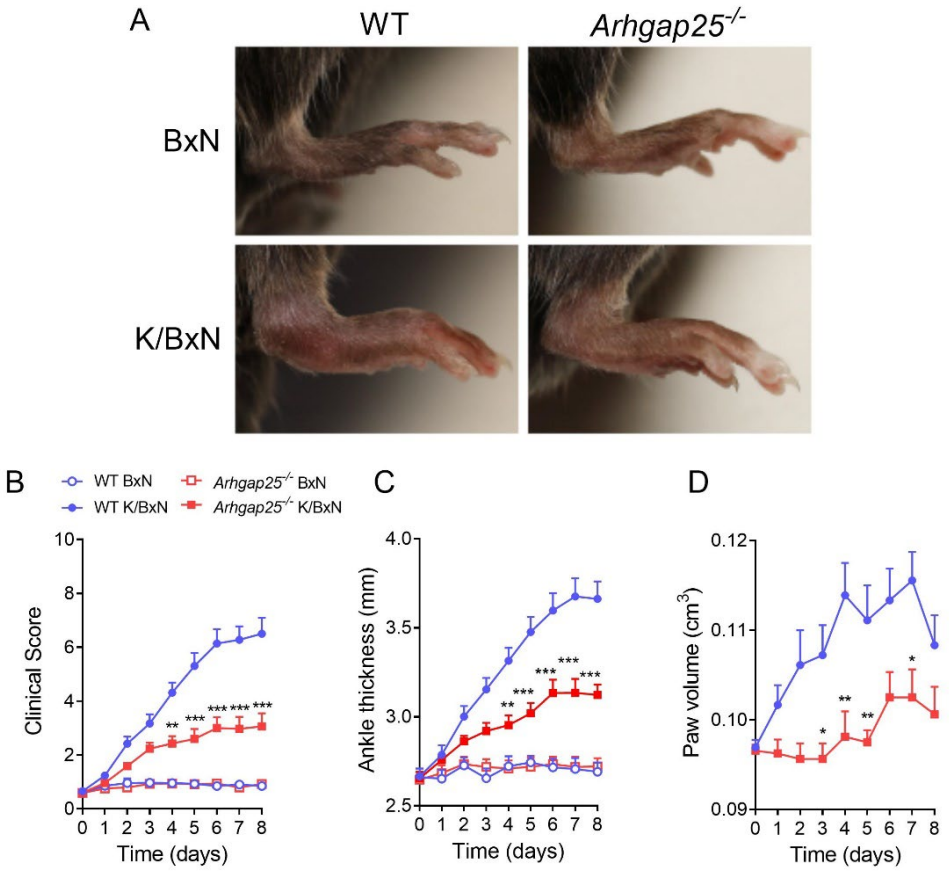

Figure 5: In the absence of ARHGAP25, the phenotypic symptoms of arthritic inflammation are significantly reduced. *WT and ARHGAP25-deficient mice were treated with arthritogenic K/BxN or, as a control, non-arthritogenic BxN serum. After 8 days, representative images of the animals' hind limbs were captured (**A**). The visible symptoms of inflammation were assessed using a semiquantitative scoring system (**B**), ankle thickness was measured using a caliper (**C**), and hind paw volume was determined with a plethysmometer (**D**) every day, for 8 days after serum treatment. Mean +SEM of 21-23 (K/BxN) or 13-14 (BxN) animals in three independent experiments are plotted. *p < 0.05, **p < 0.01, ***p < 0.001.*

4.2. Articular function is better retained, and pain-related behavior is reduced in the absence of ARHGAP25

We used the horizontal grid test to investigate the inflamed joints' possibly altered functionality. We found that ARHGAP25-deficient animals could hold on to the grid for

a significantly longer time than WT animals 3, 6, and 8 days after arthritic serum treatment (Figures 6A-C). To reveal whether this mitigated articular function deterioration in KO animals is associated with reduced pain-related behavior, we measured touch sensitivity using dynamic plantar aesthesiometry. As expected, K/BxN serum treatment resulted in a substantial decrease of the mechanonociceptive threshold in the WT animals compared to control serum-treated WT. This difference was significant after 3 days and further increased after 6 and 8 days of arthritis induction. However, in the case of ARHGAP25 KO animals, the difference between BxN-treated and K/BxN-treated mice became significant only after 8 days. Furthermore, KO arthritic mice had a significantly higher mechanonociceptive threshold compared to WT arthritic ones on days 3, 6, and 8, demonstrating the reduced pain-related behavior in the absence of ARHGAP25 (Figures 6D-F).

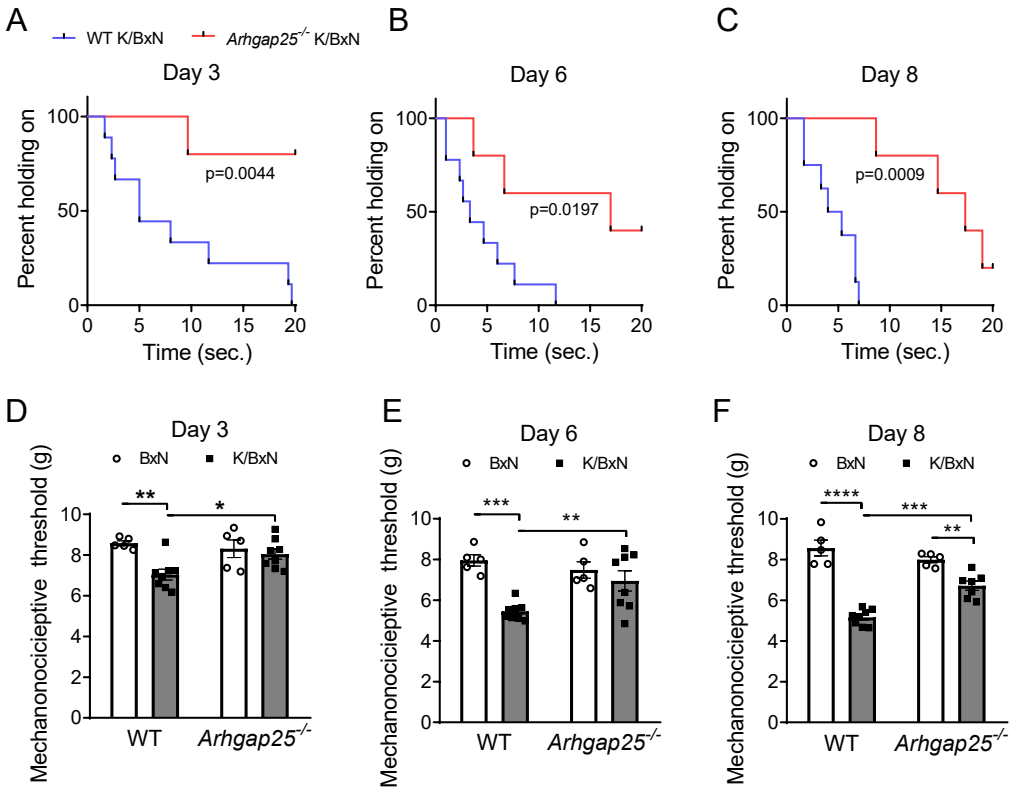

Figure 6: Griping ability is increased, while touch sensitivity is reduced in ARHGAP25-deficient mice after arthritis induction. *Articular function was measured with horizontal grid test and was evaluated using Kaplan-Meier survival analysis 3 (**A**), 6 (**B**), and 8 days*

*(**C**) after arthritic serum treatment. N=7-8 mice per group. Sensitivity to mechanical stimulus was assessed using a dynamic plantar aesthesiometer (DPA), 3 (**D**), 6 (**E**), and 8 days (**F**) after arthritis induction. Mean ±SEM of 8 (K/BxN) or 5 (BxN) mice are plotted. *p < 0.05, **p < 0.01, ***p < 0.001.*

4.3. ARHGAP25-deficient animals are partially protected against joint destruction

Histology of the harvested ankles was carried out 8 days after arthritis induction. Analyzing the hematoxylin and eosin-stained sections, extensive fibroblast-like synoviocyte accumulation with strong synovial hyperplasia was detectable in WT arthritic animals (Figure 7A, asterisk), compared to control WT, while the K/BxN-treated KO animals showed only moderate changes compared to control (Figure 7A). Semiquantitative scoring of the sections revealed that although synovial hyperplasia was present in arthritic serum-treated KO animals, it was significantly less severe compared to the treated WT mice (Figure 7B). Moreover, Safranin O staining showed considerable collagen deposition in WT arthritic animals, which decreased in the KO arthritic mice as well (Figure 7A, C). Remarkably, cartilage destruction was completely absent in KO K/BxN serum-treated mice in contrast to WT arthritic animals, where considerable cartilage destruction was detected (Figures 7A arrows, D).

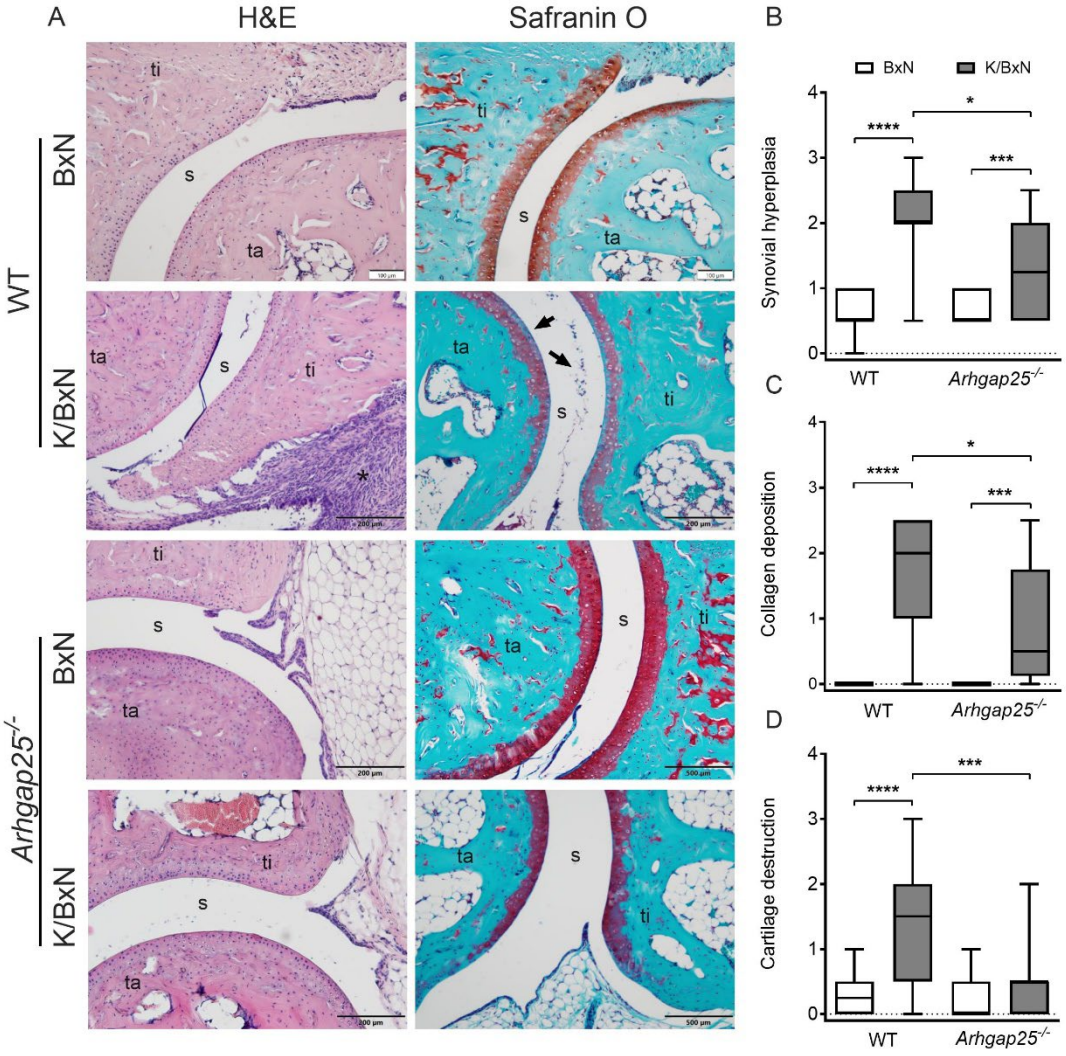

Figure 7: Joint destruction is reduced in the absence of ARHGAP25. *Ankle sections were prepared and stained with H&E or Safranin O**,** and images were captured (ta: tarsus, ti: tibia, s: synovium) (**A**). In the ankle joints of arthritic WT mice, synovial fibroblasts become hyperactive and rapidly proliferate, causing the characteristic synovial hyperplasia (**A**, asterisk). Cartilage destruction was observable in WT animals after arthritis induction (**A**, arrows). Box plots represent the semiquantitative histopathological scores of synovial hyperplasia (**B**), collagen deposition (**C**) and cartilage destruction scores (**D**) of 16-19 (K/BxN) or 10-12 (BxN) animals. *p < 0.05, ***p < 0.001.*

4.4. Neutrophil effector mechanisms are not affected by the absence of ARHGAP25 in the K/BxN STA model

Since the K/BxN serum transfer arthritis model is highly dependent on the innate arm of immunity, and neutrophilic granulocytes have a crucial role in the development of arthritis in this model, we set out to investigate two important, connected effector functions of these cells, the myeloperoxidase (MPO) activity in vivo, and the superoxide production in vitro. Figure 8A shows the representative pictures of MPO activity measurements in the hind paws, one, two, and seven days after arthritis induction. We found that treatment with K/BxN serum increased the MPO activity to a similar extent in both groups. Although slightly decreased MPO activity in KO animals compared to WT was observed one day after arthritis induction, this difference disappeared on day two and was not detected on day 7 either (Figures 8B-D). For the in vitro superoxide production measurement, neutrophilic granulocytes were isolated from the bone marrow of non-treated WT and KO animals, and three different stimulations were used to induce the release of superoxide: HSA-anti-HSA immune complex surface, PMA (a pharmacologic stimulator), and integrin surface combined with TNFα activation. In all three cases, the amount of superoxide released was similar between KO and WT neutrophils, and no significant difference was observable (Figures 8E-G).

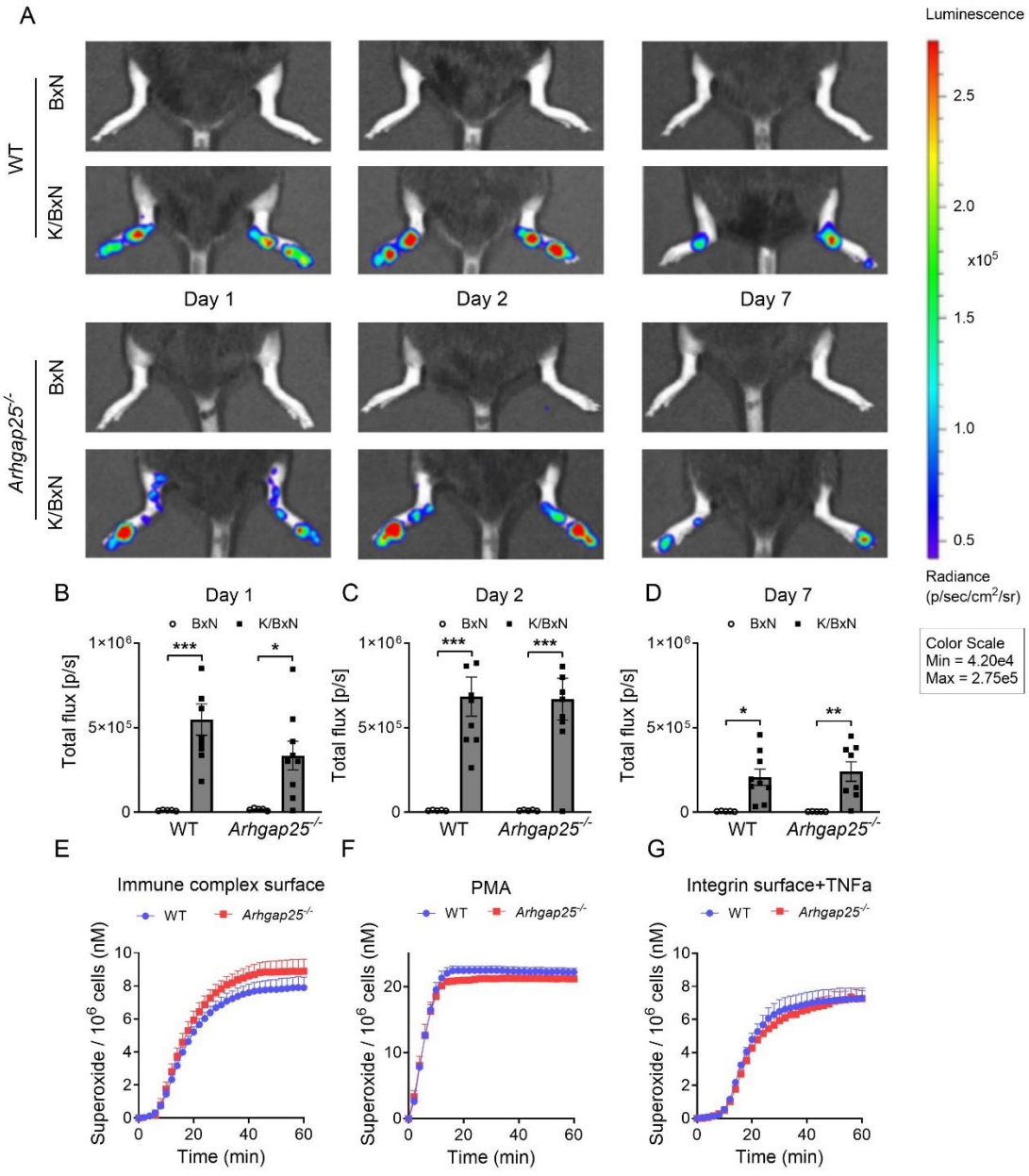

Figure 8: In this model, the in vivo MPO activity and the in vitro neutrophil superoxide production are not affected by the deletion of ARHGAP25*. Neutrophil MPO activity in the ankles of animals was assessed using the IVIS Lumina III In Vivo Imaging System one (**A, B**), two (**A, C**), and seven days after arthritis induction (**A, D**). Mean ±SEM of 9 (K/BxN) or 5 (BxN) mice are plotted. Superoxide release of bone marrow-derived neutrophils was measured in vitro by cytochrome C reduction assay, upon immune complex (**E**), PMA (**F**), or integrin surface (**G**) stimulus. Mean +SEM of 4-5 animals is shown. *p < 0.05, **p < 0.01, ***p < 0.001.*

4.5. Deletion of ARHGAP25 results in decreased leukocyte recruitment and inflammatory cytokine levels in the inflamed ankles

Flow cytometry was used to measure the infiltration of neutrophils and macrophages into the inflamed ankle joints of animals. As expected, K/BxN serum administration induced strong recruitment of Ly6G+ neutrophils and F4/80+ macrophages into the synovium of WT animals. However, in ARHGAP25-deficient animals, neutrophil infiltration was reduced by approximately a third (Figure 9A) while macrophage infiltration was roughly halved compared to WT (Figure 9B). Since this observed difference in leukocyte recruitment might be the result of an altered cytokine environment in the KO animals, we decided to investigate possible changes in the amount of two relevant cytokines: IL-1β, which is an essential regulator of inflammation, and MIP-2, which is important for leukocyte infiltration (127-129). Although in both genotypes, the amount of both cytokines was strongly elevated by arthritic serum treatment, in the case of ARHGAP25-deficient animals, IL-1β and MIP-2 concentration were approximately a third of what was measured in WT animals, suggesting an altered inflammatory environment in KO animals (Figure 9C, D).

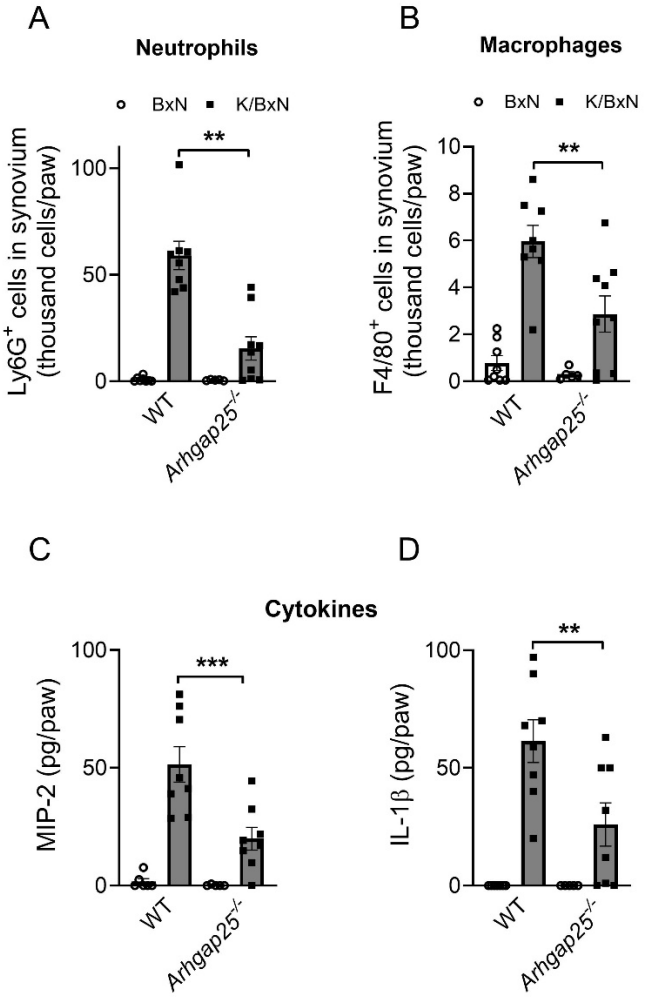

Figure 9: Phagocyte infiltration and inflammatory cytokine production is reduced in the synovial infiltrate of ARHGAP25-deficient animals. *Five days after serum injection, the synovium of mice was flushed, and the inflammatory infiltrate was analyzed. Flow cytometry was used to measure neutrophil (**A**), and macrophage numbers (**B**). Mean ±SEM of 9-10 (K/BxN) or 5-8 (BxN) mice are plotted. IL-1β (**E**) and MIP-2 (**F**) amounts in the synovial infiltrate were determined with sandwich ELISA. Mean ±SEM of 8 (K/BxN) or 5-7 (BxN) mice are plotted. **p < 0.01, ***p < 0.001.*

4.6. Lacking ARHGAP25 likely affects the ERK-MAPK, the NF-κB-IκB, and the E-cadherin signaling pathways in the K/BxN serum transfer arthritis model

To reveal which signaling pathways are responsible for the observed effects of ARHGAP25 in autoantibody–induced arthritis, a comprehensive western blot analysis was conducted using total hind paw lysates. The expression of ERK1/2, MAPK, NF-κB, I-κB, E-cadherin, and β-catenin, as well as the phosphorylated forms of these proteins, where it was relevant, was investigated (Figure 10A). Densitometric evaluation revealed that in WT animals, K/BxN serum treatment resulted in a remarkable increase in total I-κB expression, which was completely absent in ARHGAP25 KO animals (Figure 10B). Parallelly, arthritic serum treatment resulted in an increased tendency of total NF-κB. These results suggest that ARHGAP25 may be involved in regulating NF-κB through I-κB. Similarly, the expression of total MAPK was elevated in arthritic WT animals compared to KO, which was in accordance with the changes in total ERK1/2. Total E-cadherin was also significantly increased upon treatment in WT compared to KO mice, while in the case of β-catenin, only an increased tendency was observable (Figure 10B).

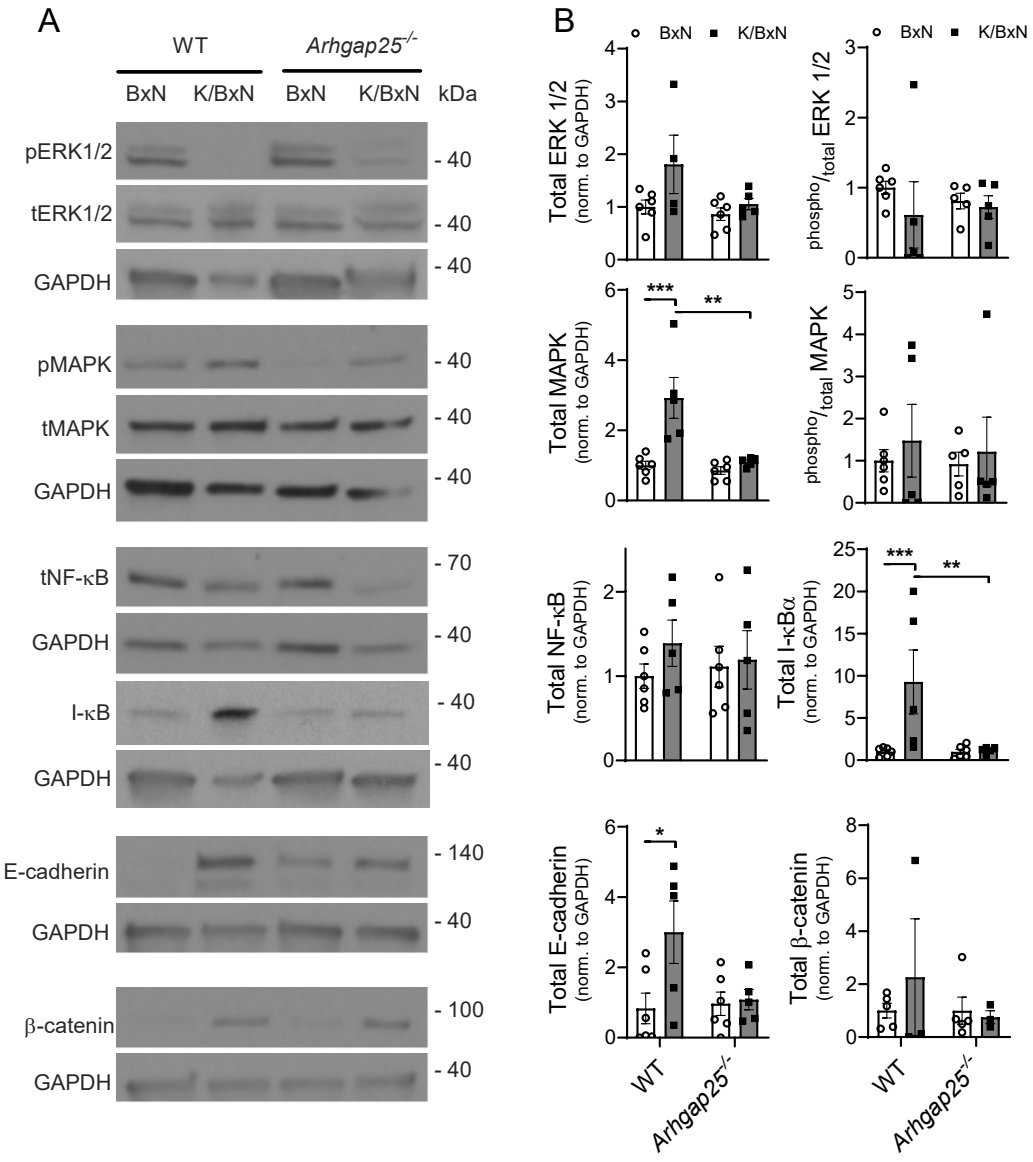

Figure 10: Comprehensive western blot analysis of the different signaling cascades possibly affected by ARHGAP25 deletion in the K/BxN STA model. *WT and ARHGAP25-deficient mice were sacrificed five days after arthritis induction. Afterward, the ankles were harvested, snap-frozen, lysed, and used for a series of western blot experiments. Representative blots are shown for the MAPK/ERK, NF-κB, and WNT/β-catenin pathways (**A**). Densitometric analysis of the western blots (**B**). Mean ±SEM of 4-6 mice per group are plotted. **p < 0.01, ***p < 0.001.*

4.7. In bone marrow chimeric mice, moderate mitigation of arthritic inflammation was observable

Next, we were curious whether the observed inflammatory effect of ARHGAP25 in autoimmune arthritis is due to only hematopoietic cells or may other cell types be involved. To investigate this, three types of bone marrow chimera animals were generated. "Normal chimeras" carry ARHGAP25-deficient hematopoietic compartment on WT background (*Arhgap25*$^{-/-}$→WT). In "reverse chimeras", hematopoietic cells are WT, but all other cells lack ARHGAP25 (WT→*Arhgap25*$^{-/-}$). As a control, "WT chimeras" (WT→WT) were used with WT hematopoietic cells on a WT background (of a different animal). Then, arthritis was induced in these mice, and clinical score, ankle thickness, and grid tests were performed. Interestingly, in "normal chimeras" (*Arhgap25*$^{-/-}$→WT), we found only a moderate decrease in clinical score and ankle thickness compared to the chimeras carrying the WT hematopoietic cells on WT background (WT→WT) after K/BxN serum treatment. From day 7, this decrease became significant (Figure 11A, B). Similar results were obtained using "reverse chimeras" (WT→*Arhgap25*$^{-/-}$). In these animals, ankle thickness was significantly reduced from day 6 compared to WT chimeras (WT→WT), but in the clinical score, only a decreased tendency and no significant difference was detected (Figure 11D). Articular functions were slightly but not significantly better retained in both "normal" and reverse chimeras (*Arhgap25*$^{-/-}$→WT and WT→*Arhgap25*$^{-/-}$, p=0.88072 and p=0.769, respectively) compared to WT chimeras (Figure 11C, F). Based on these data, we suspect that ARHGAP25 is involved in the pathomechanism of autoimmune arthritis by regulating both hematopoietic and non-hematopoietic cells.

4.8. Fibroblast-like synoviocytes have a strong ARHGAP25 expression, similar to neutrophils

Fibroblast-like synoviocytes are very important in disease development and progression in autoimmune arthritis. As we suspected that these non-hematopoietic cells might be involved in the observed decrease of disease severity in ARHGAP25-deficient animals, we decided to investigate the expression of ARHGAP25 protein in fibroblast-like synoviocytes derived from arthritogenic serum-treated WT animals. Surprisingly, western blot experiments revealed robust expression in these cell types, comparable to that found

in neutrophils (Figure 11G). However, mouse embryonic fibroblast cells showed only a weak signal, which suggests that the high expression is specific to fibroblast-like synoviocytes and not present in other types of fibroblasts. Fibroblast-like synoviocytes isolated from KO arthritic mice were used as negative control (Figure 11G).

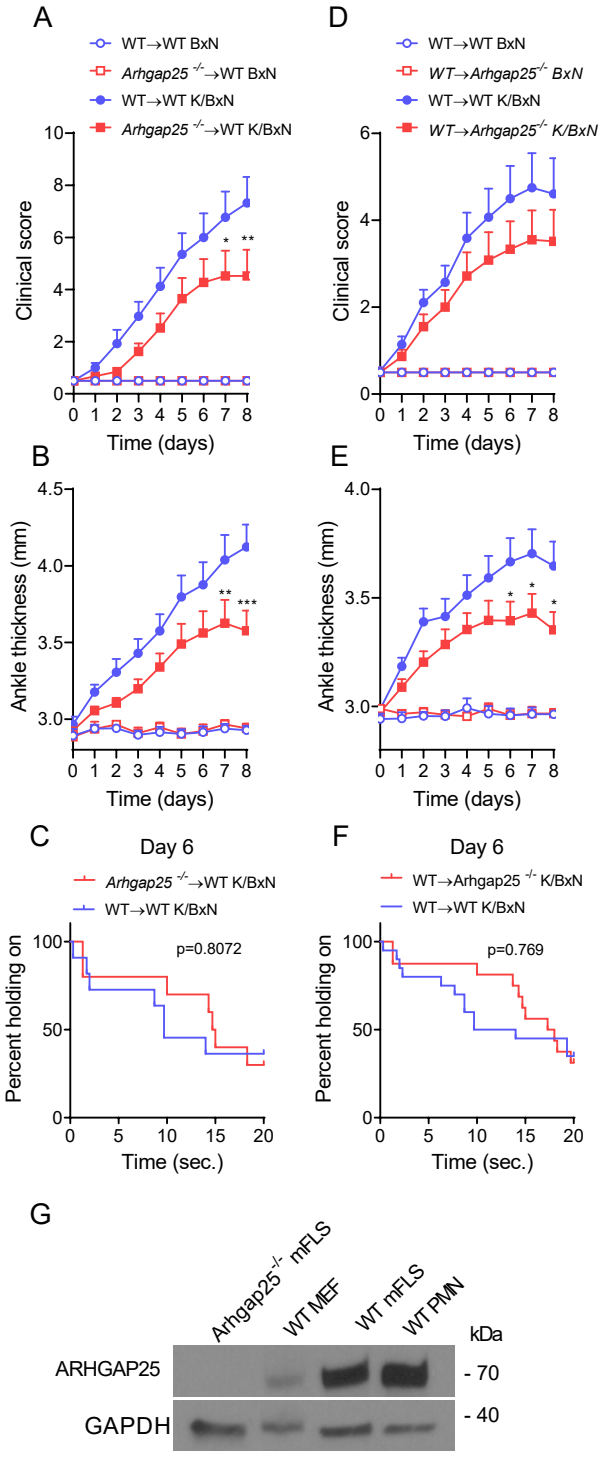

Figure 11: Mitigated inflammatory phenotype in the case of both normal and reverse KO bone marrow chimeras was observed. *Animals were created with ARHGAP25 expression either only in cells of the hematopoietic lineage (WT→Arhgap25$^{-/-}$, or reverse chimeras) or in all cells besides the hematopoietic compartment (Arhgap25$^{-/-}$→ WT, or*

*"normal" chimeras). After treatment of these animals with arthritogen, or control serum, clinical severity and ankle thickness were assessed for 8 days (**A, B, D, E**). Mean +SEM of 10-15 (K/BxN) or 6 (BxN) animals are shown in two independent experiments. Joint function deterioration was assessed with horizontal grid test in both types of bone marrow chimeras (**C, F**). Fibroblast-like synoviocytes were isolated and cultured from the harvested ankles of arthritic mice, and lysates of the mFLS were separated by SDS-PAGE. A representative western blot revealed high ARHGAP25 expression in fibroblast-like synoviocytes (**G**). (mFLS: mouse fibroblast-like synoviocytes, MEF: mouse embryonic fibroblasts, PMN: Polymorphonuclear neutrophils.) *p < 0.05, **p < 0.01, ***p < 0.001.*

4.9. ARHGAP25 expression is elevated by ACD in humans and by CHS in mice

Although several studies reported that in tumor tissues, ARHGAP25 expression can be altered (75, 77, 78), there is no evidence whether similar changes in expression occur in inflammatory diseases. For this reason, we decided to investigate ARHGAP25 expression in human samples harvested from healthy and inflamed skin areas of patients suffering from ACD. We used RT-qPCR and WB techniques to assess the expression at both the mRNA and protein levels. Interestingly, we found that inflamed skin samples showed significantly higher mRNA (Figure 12A) and protein expression than healthy samples collected from the same patients (Figure 12C, D). We wanted to implement this measurement in our contact hypersensitivity model. For this, WT animals were treated with either TNCB or vehicle on their shaved abdomen, and five days later, the ears of both groups were painted with TNCB. In those mice, which received TNCB twice (on both the abdomen and the ears), the elicitation phase of CHS is initiated in the ears. In mice that received TNCB treatment only to the ears, the sensitization phase was triggered. RT-qPCR and WB experiments revealed that elicitation with the allergen significantly increased the mRNA and protein level of ARHGAP25 compared to only sensitized ears (Figure 12B, C, E). These changes were analogous to the ones observed in human samples, thus we decided that this disease model is suitable for further investigation of the role of ARHGAP25 in contact hypersensitivity. It is known that ARHGAP25 is highly expressed in leukocytes, but there are also reports of its expression in several other cell types (75, 77, 78, 80, 81). This prompted us to investigate the presence of ARHGAP25 in the epidermis of WT ears. Since we found no detectable mRNA or protein expression

in the epidermis of either sensitized or elicited ears, we concluded that keratinocytes do not express this protein in either phase of the allergic reaction (Figure 12B, C, E).

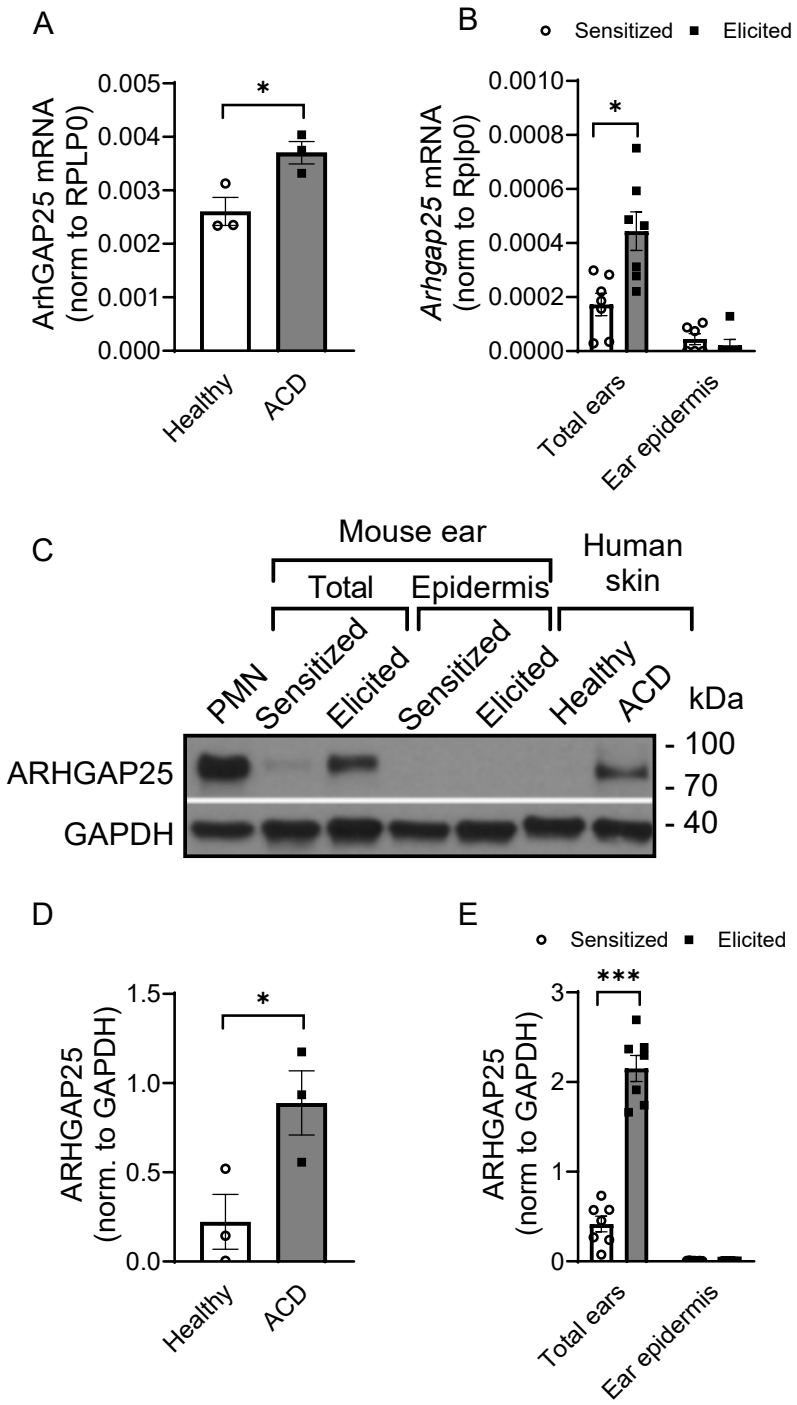

Figure 12: ARHGAP25 is overexpressed in ACD in humans and in the elicitation phase of CHS in mice. *ARHGAP25 expression was measured in skin samples of human patients with RT-qPCR on the RNA level (**A**) or with western blot on the protein level (**C**).*

*Densitometric evaluation of the western blots (**D**). Similarly, ARHGAP25 expression was assessed in total ear samples of sensitized or elicited mice, and in the epidermis of ears using RT-q PCR (**B**), or western blot (**C, E**). Mean ±SEM of 7 mice, and 3 human samples per group are plotted *p<0.05, ***p<0.001.*

4.10. In the case of allergic contact hypersensitivity, the lack of ARHGAP25 results in decreased inflammation

The promising results with the K/BxN serum arthritis model and the above-described expression changes in ACD prompted us to investigate the role of ARHGAP25 in the TNCB-induced allergic contact hypersensitivity model. To this end, we treated WT, ARHGAP25-deficient mice, and "normal" bone marrow chimeras (*Arhgap25*$^{-/-}$→WT and WT→WT) with TNCB on the abdomen and the ears (or only the ears) as described previously. Histology revealed substantial leukocyte accumulation in WT ears, which was reduced in the case of the ARHGAP25 KO animals (Figure 13A). Five days after abdomen, but before ear treatment, no difference in ear thickness was measured between KO and WT (Figure 13A, B) or KO chimera (*Arhgap25*$^{-/-}$→WT) and WT chimera (WT→WT) mice in either treatment group (Figure 13E). Similarly, ear thickness, or ear thickening was unchanged between KO and WT, in animals that were only sensitized with the allergen on the ears. However, the second TNCB treatment resulted in remarkable ear thickening in WT animals, which, interestingly, was significantly lower in the case of KO mice (Figure 13A, C, D). Similarly, we observed a substantially lower ear thickness and a milder ear thickening in KO chimeras compared to WT chimeras (Figure 13F, G).

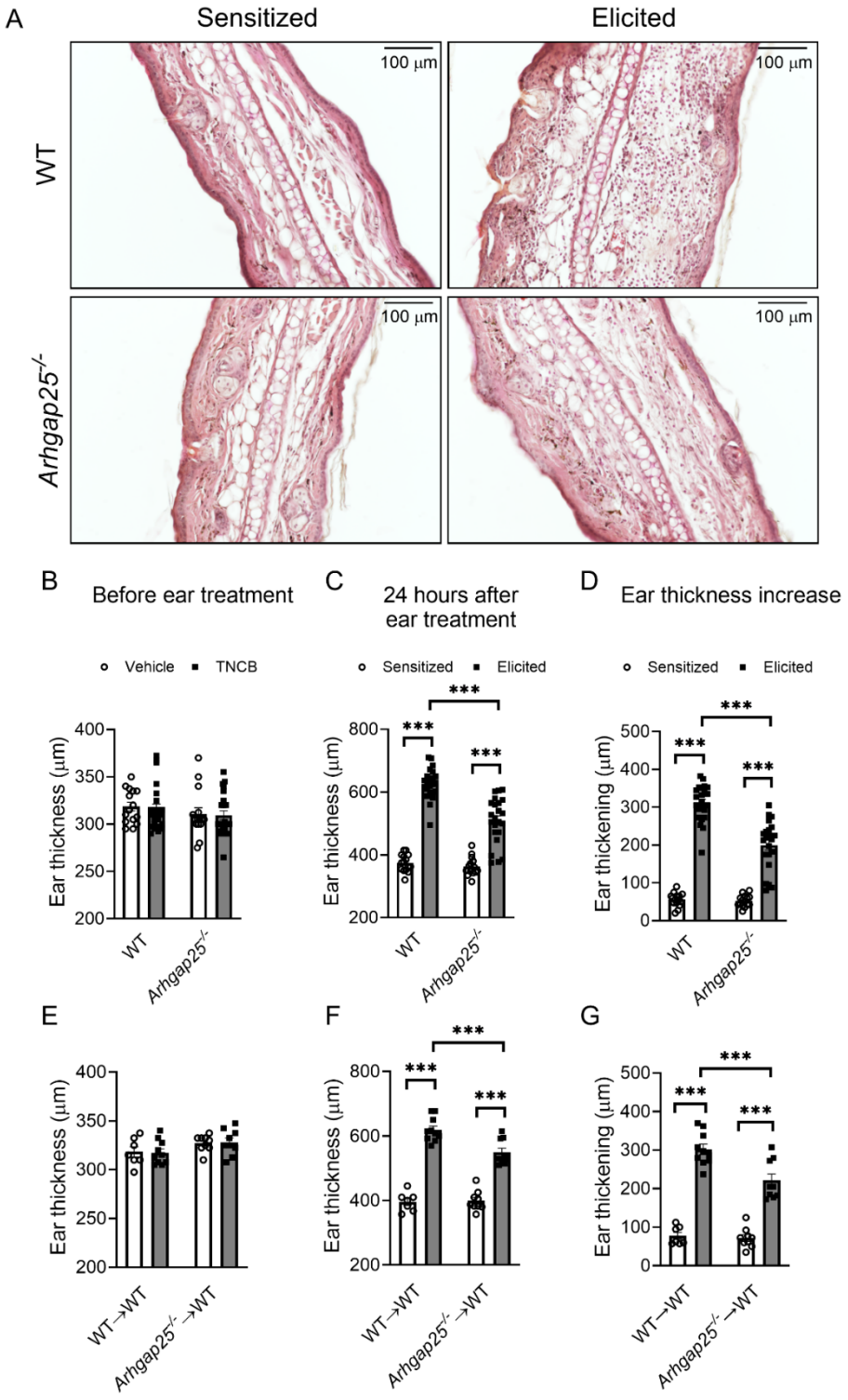

Figure 13: Allergic ear swelling is mitigated in the absence of ARHGAP25. *Mice were either sensitized, or elicited to the contact hypersensitivity reaction on the ears. twenty-four hours later, ear sections were prepared and stained with hematoxilyn and eosin (**A**).*

*Prior to ear treatment, ear thickness was measured, of total WT and KO (**A, B**) or "normal" WT and KO bone marrow chimera animals (**E**). Twenty-four hours after coating the ears with the allergen ear thickness was measured again in total WT and KO (**C**), and or chimeric mice (**F**). Afterwards, ear thickness increase was calculated (**D, G**). Mean ±SEM of 9-17 animals is plotted in three independent experiments in case of full WT and KO or 5-10 in two independent experiments in case of chimeras, ***p<0.001.*

4.11. In the elicitation phase of contact hypersensitivity, infiltration of phagocytes and T cells is reduced in *Arhgap25*$^{-/-}$ mice

Next, we decided to test whether the previously observed, decreased leukocyte recruitment to the inflamed tissue in the case of KO animals in autoimmune arthritis could be detected in the ACH model as well. To achieve this, 24 hours after the TNCB challenge, mice were sacrificed, ears were harvested, the connective tissue was lysed, and cells were labeled with specific antibodies. Flow cytometric measurements revealed that in case of WT animals second exposure to the allergen resulted in significant leukocyte (CD45+ cells), myeloid leukocyte (CD45+CD11b+ cells), neutrophil (CD45+CD11b+Ly6G+ cells) and macrophage (CD45+CD11b+F4/80+ cells) infiltration to the ears compared to only sensitized animals. In the case of *Arhgap25* KO mice, this difference between sensitized and elicited ears was not significant (Figure 14A, B, C, D). When we compared the number of different leukocytes in the elicited ears of WT and KO mice, we found, significantly lower leukocyte, myeloid leukocyte and macrophage numbers in KO, while neutrophil recruitment had only a decreased tendency (Figure 14A, B, C, D).

In parallel with the myeloid cells, the numbers of different subpopulations of T cells were measured in the ears of the animals with flow cytometry. In WT mice, elicitation of the allergic reaction resulted in increased total T cell (CD45+CD3+), and specifically T helper (CD45+CD3+CD4+) and cytotoxic T cell (CD45+CD3+CD8+) recruitment (Figure 14E, F, G). The comparison of WT and KO animals that were elicited with TNCB shows that total T cell and especially cytotoxic T cell infiltration is significantly reduced in the absence of ARHGAP25 (Figure 14E, F, G)

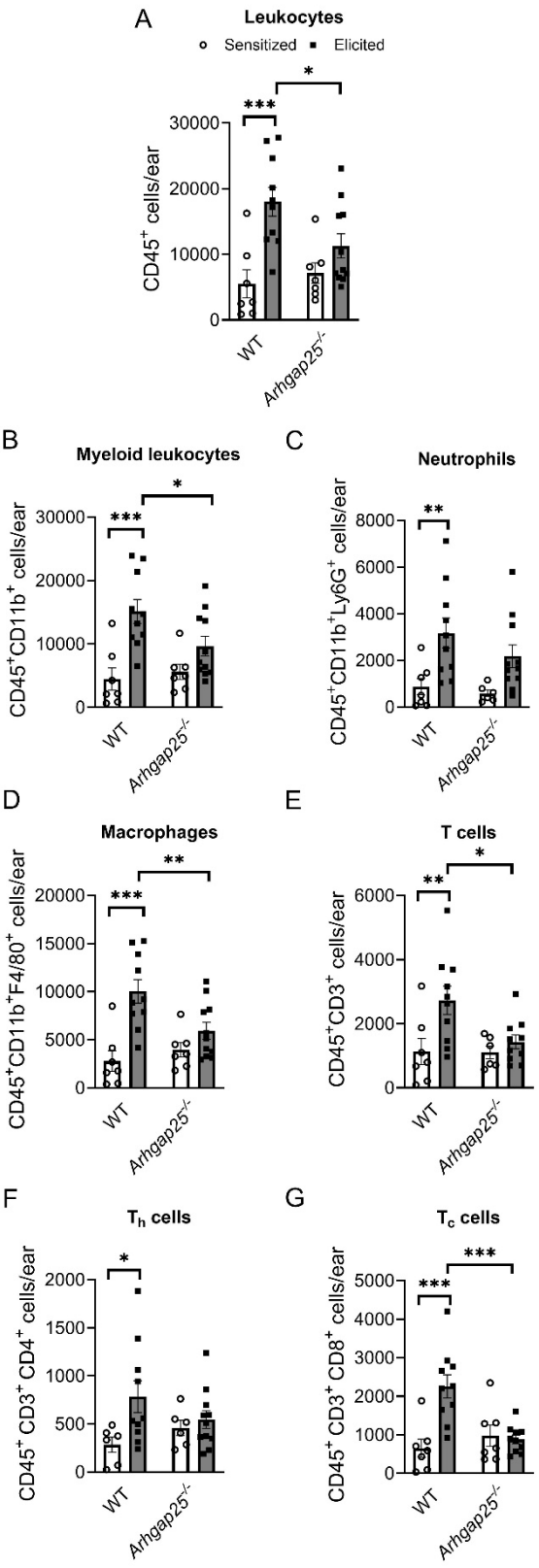
A
Leukocytes
Sensitized
Elicited
CD45+ cells/ear
B
Myeloid leukocytes
CD45+CD11b+ cells/ear
C
Neutrophils
CD45+CD11b+Ly6G+ cells/ear
D
Macrophages
CD45+CD11b+F4/80+ cells/ear
E
T cells
CD45+CD3+ cells/ear
F
Th cells
CD45+ CD3+ CD4+ cells/ear
G
Tc cells
CD45+ CD3+ CD8+ cells/ear
WT
Arhgap25-/-

Figure 14: The lack of ARHGAP25 decreased the phagocyte and T cell recruitment to the site of allergen exposure. *One day after TNCB treatment, the connective tissue of the ears of wild type and ARHGAP25 knockout mice were digested with Liberase enzyme cocktail. Following specific staining the numbers of infiltrated total leukocytes (**A**), myeloid cells (**B**), neutrophils (**C**) and macrophages (**D**) were determined with flow cytometry. Similarly, total T cell (**E**), helper T cell (**F**), and cytotoxic T cell numbers (**G**) were measured in the ears. Mean ±SEM of 6-11 mice per group in three independent experiments are plotted. *p<0.05, **p<0.01, ***p<0.001.*

4.12. Genetic deletion of ARHGAP25 alters the cytokine milieu in the allergen-treated ears, which leads to reduced transmigration of neutrophils

The observed alteration in leukocyte recruitment to the ear tissue raises the possibility that ARHGAP25 could modify the cytokine composition. To investigate this, first, pooled supernatant samples of the digested allergen-treated ears were measured by cytokine array. We found that soluble ICAM-1, C5/C5a, IL-1α, and TIMP-1 signals were similarly high in mice that received allergen treatment once or twice in both genotypes (Figure 15 A, B, C). CCL2 and IL-1ra levels were moderately high in sensitized animals, and their signal further increased by eliciting the allergic reaction. In the case of many CXCL and CCL chemokines, e.g., MIP-2/CXCL2, CCL4, CCL9, CCL5, CCL3, CCL12, but also in the case of IL-1β, sensitization did not result in detectable signal. However, in the elicitation phase relatively high level could be measured in both genotypes, although it was lower in KO than in WT samples (Figure 15 A, B, C). CXCL1 and CXCL12 expressions seem to be slightly lower in the sensitization phase in ARHGAP25-deficient mice than in WT, but in the elicitation phase, they show similar levels in the two genotypes. IL-16 and TREM1 signals were augmented by the second encounter with the allergen in WT and KO, but were lower in both phases in KO samples (Figure 15 A, B, C). In the case of several interleukins, e.g., IL-17, IL-7, and IL-27, but also in IFN-γ, high levels were measured in the sensitization phase in WT ears. In the elicitation phase, their expression diminished, while in KO mice, no signal was detected in either phase. M-CSF expression seems to be relatively high in both phases of the allergic reaction in WT but not in KO animals (Figure 15 A, B, C).

IL-1β and MIP-2/CXCL2, that proved to be modified by ARHGAP25 in autoantibody-induced arthritis were also measured in this model with ELISA. In the elicited ear

samples, the amount of IL-1β significantly increased both in WT and KO. However, its concentration was lower in KO than in the WT animals (Figure 15 D). Although MIP-2 showed a similar pattern, no significant difference between KO and WT could be detected after the second encounter with the allergen. However, the elicitation caused a significant increase in MIP-2 concentration only in WT, but not in KO mice (Figure 15 E).

Next, to investigate whether the differences in leukocyte infiltration are the result of the alterations in the cytokine milieu, in vitro transwell assay was performed, using bone marrow derived PMN and cell-free supernatants of the digested ear samples. Looking at the transmigration capacity of KO and WT neutrophils towards the same supernatant, no difference is observable between ARHGAP25-deficient and WT neutrophils. However, PMN isolated from both genotypes transmigrated in a significantly higher ratio towards supernatant earned from the elicited ears of WT mice, compared to sensitized ones. On the other hand, not such elevation in migrating capability was measured towards elicited supernatants from KO animals compared to sensitized ones. Importantly, both KO and WT neutrophils showed significantly decreased migration towards supernatant of elicited KO, then towards supernatant of elicited WT mice (Figure 15 F).

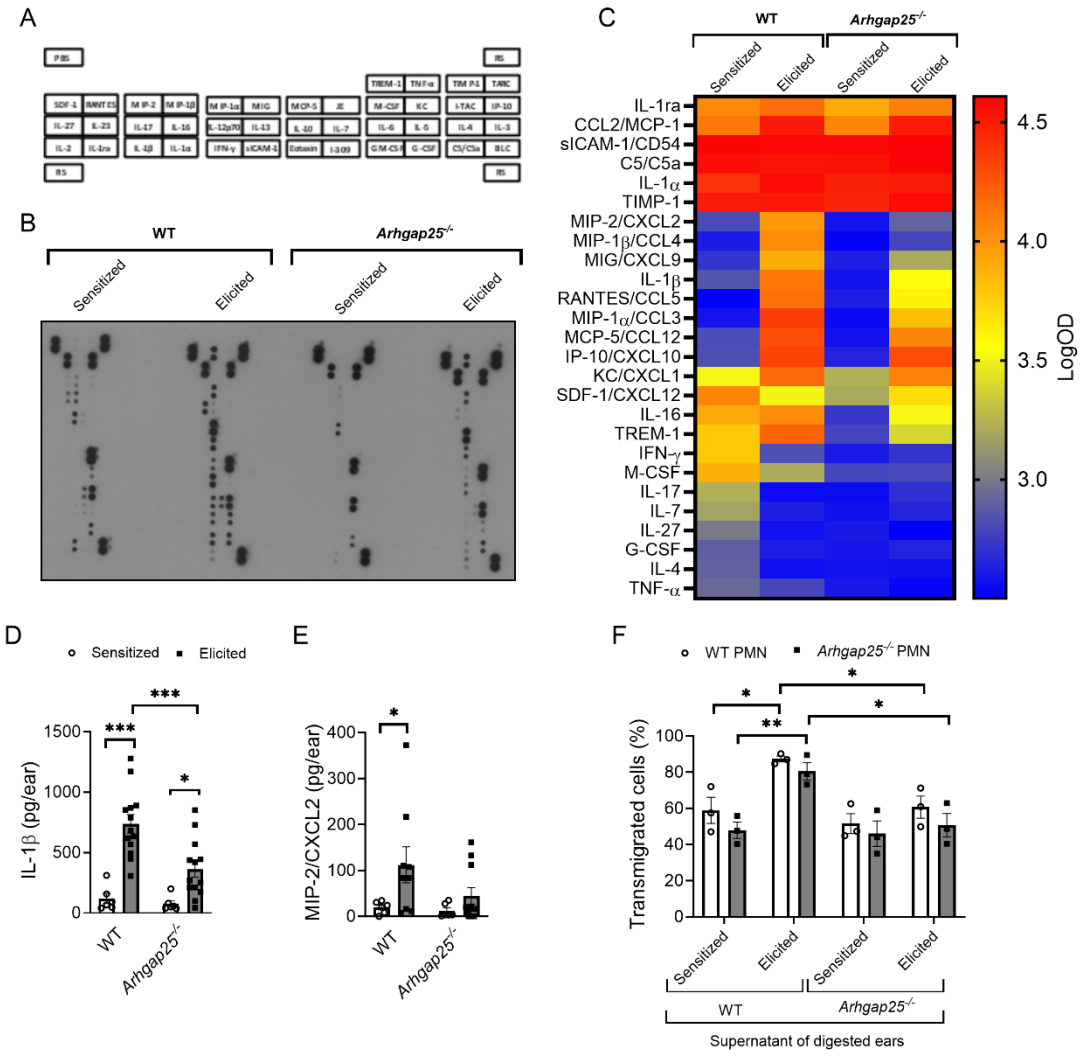

Figure 15: Lacking ARHGAP25 altered the cytokine profile in both phases of the allergic reaction. *Cytokine array and ELISA measurements were conducted from the digested ears' supernatants. The layout of cytokines on the cytokine array in duplicates is indicated (**A**). Image of a film developed from the cytokine array (**B**). A heat map was constructed of the integrated pixel densities of cytokines that appeared on the array in a logarithmic scale (**C**). Quantitative, sandwich ELISA measurement of IL-1β (**D**) and MIP-2 concentrations (**E**). In vitro transmigration assay of PMN, isolated from WT or KO mice was conducted towards supernatants earned from the allergen-treated ears of WT or KO animals (**F**). Cytokine array and transwell assay were measured using pooled samples of 9 animals in each experimental group. Mean ±SEM of 6-13 mice per group are plotted in*

*the case of the ELISA experiments, and 3 in the case of transwell assay, *p<0.05, **p<0.01, ***p<0.001.*

4.13. ARHGAP25 does not affect T cell activation and homing in the draining lymph nodes after sensitization

The above-described alteration in cytokine composition in the sensitization phase of CHS raises the possibility that T cell activation and homing to the draining lymph nodes could be altered by ARHGAP25. To investigate this, mice were treated with either TNCB or only vehicle on the abdomen, and the inguinal and axillary lymph nodes were excised. Then, cells were isolated, and flow cytometry was conducted. We found that in both genotypes, sensitization increased the helper ($CD3^+CD4^+$), and cytotoxic ($CD3^+CD8^+$) T cell counts in the lymph nodes however, the differences were statistically not significant (Figure 16A, B).

We also measured the activation state of T cells. For this we labelled alpha subunit of the IL-2 receptor (CD25), which is considered to be a late activation marker of lymphocytes, and the transmembrane C-type lectin protein (CD69), an early activation marker of T cells (130). The ratio of CD25 expressing $CD4^+$ helper T cells was significantly elevated after sensitization, while within CD8+ cytotoxic T cells, only a moderate increase in CD25 expression was detected. The CD69 expressing cell number was significantly higher within both $CD4^+$ helper and $CD8^+$ cytotoxic T cell subtypes compared to unsensitized control. However, the absence of ARHGAP25 did not cause any difference in the expression of either activation marker (Figure 16C-F).

Next, we wanted to reveal whether ARHGAP25-deficient cells obtained from the draining lymph nodes could induce the previously observed ear thickening reduction (compared to WT cells) in WT animals. Therefore, cells were isolated from the inguinal and axillary lymph nodes of sensitized WT and ARHGAP25-deficient mice and injected into untreated WT and KO animals. This should initiate sensitization in the recipient mice. Afterward, the ears were painted with the allergen, as an elicitation step, and ear thickness was measured as we described previously. Our results show that considerable ear thickness increase was induced in KO lymph node-derived cell receiving WT recipient (*Arhgap25*$^{-/-}$→WT), and WT lymph node-derived cell receiving WT mice (WT→WT). However, in KO-recipient animals receiving WT lymph nodal cells (WT→*Arhgap25*$^{-/-}$)

ear thickening was significantly reduced compared to the other two experimental groups (Figure 16G).

These results indicate that T cell homing and activation in the sensitization phase of CHS is not affected by ARHGAP25, but rather the elicitation phase is regulated.

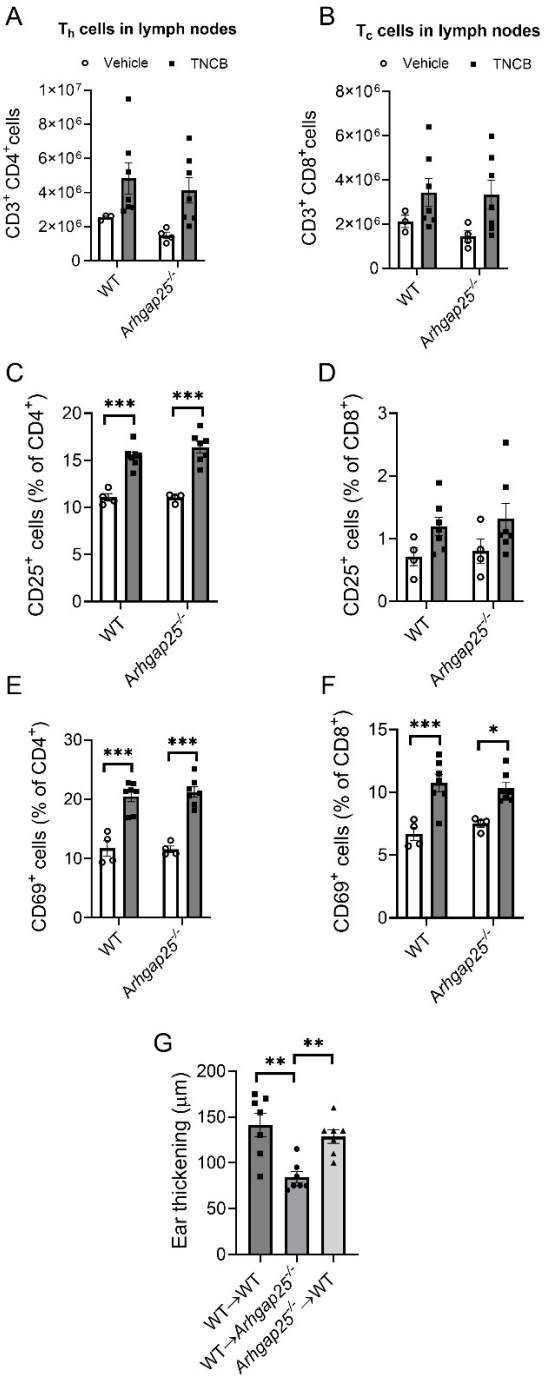

Figure 16: In the sensitization phase, T cell homing and activation in the lymph nodes are not affected by ARHGAP25. *Draining lymph nodes of mice were harvested five days*

*after allergen treatment of the abdominal skin. Samples were homogenized, filtered, and cells were labeled for different T cell-specific (CD3, CD4, and CD8) and T cell activation markers (CD25 and CD69). T helper (**A**) and cytotoxic T cell numbers were determined with flow cytometry (**B**). The ratio of activated T helper and cytotoxic T cells was assessed via CD25 (**C, D**) and CD69 positivity (**E, F**). Lymph node-derived cells of allergen-treated mice were transferred into resting animals for sensitization, and ear thickness was measured before and 24 hours after TNCB treatment of the ears (**G**). Mean ±SEM of 3-7 mice per group in two independent experiments are plotted. *p<0.05, **p<0.01, ***p<0.001*

5. DISCUSSION

Our research group focuses on the GTPase-activating protein ARHGAP25 and cloned the full-length protein for the first time in 2012. With the use of in vitro methods and experiments carried out with various cell lines, it was demonstrated that through the modulation of RAC small G protein, ARHGAP25 is an essential regulator of neutrophil effector functions such as phagocytosis and superoxide production (68, 69). Our research group also purchased an ARHGAP25-deficient mouse strain and, using these animals, demonstrated that the protein is involved in the complex regulation of trans-endothelial migration of leukocytes (70). Although initially it was believed that this protein is expressed only in leukocytes, recently, an increasing number of publications have demonstrated regulatory roles of ARHGAP25 in diseases of non-hematopoietic origin, mainly in different types of cancer (75-78). It should be noted that even though the expression of ARHGAP25 is substantially weaker in tumor cells than in leukocytes, it seems that it is still crucial in the regulation of metastasis. It is also interesting, that in the case of different types of tumor development, the expression of ARHGAP25 can be altered, contributing to the progression of the disease. This raises the possibility, that expressional change of the protein could be involved in other pathologic conditions, especially where immune cells are key players, such as inflammatory diseases (77-79).

These findings prompted us to investigate the role of ARHGAP25 in two mechanistically different inflammatory disease models: in the K/BxN serum transfer arthritis (STA) model and the TNCB-induced allergic contact hypersensitivity model.

In the K/BxN STA model, severe joint inflammation and articular damage are developed due to the administered autoantibodies and subsequent immunologic events. Although many cell types contribute to the progression of inflammation, cells of the adaptive arm of the immune system play a minor (if any) role in this model. The most prominent cell types of the K/BxN STA model include leukocytes of the myeloid lineage, such as neutrophilic granulocytes, macrophages, and osteoclasts, and other, non-immune cells, mainly fibroblast-like synoviocytes (58).

In the TNCB-induced contact hypersensitivity model, Th and Tc cells are crucial for the development of the delayed type hypersensitivity reaction, both in the sensitization, and the elicitation phases (131, 132). In the elicitation phase of the disease, tissue damage is largely aggravated by macrophages and neutrophils similarly as in the K/BxN STA model.

Moreover, keratinocytes may also contribute to the allergic reaction by releasing various cytokines.

Interestingly we found that the lack of ARHGAP25 significantly mitigated the phenotypical symptoms of both autoantibody-induced arthritis and contact hypersensitivity. In arthritis, milder ankle swelling and clinical severity were associated with better retained joint function and decreased pain sensitivity to mechanical stimulus. Histological evaluation of the ankles of arthritic animals revealed that lack of ARHGAP25 results in reduced joint damage, which manifests in mitigated synovial hyperplasia and collagen deposition. Most notably, cartilage destruction was completely absent in KO animals, which can explain the milder symptoms and the lower pain sensation.

In inflammatory conditions, neutrophilic granulocytes release reactive compounds, such as myeloperoxidase and reactive oxygen species, into their environment. These events contribute to the elimination of pathogens, but can also damage the host tissue substantially, especially in cases of sterile inflammation, where no pathogens are present (133). To answer, what could be the reason for the milder symptoms of inflammation observed in the absence of ARHGAP25, we first chose to investigate whether neutrophil effector functions could be altered. However, surprisingly, we failed to detect significant differences in both the in vivo myeloperoxidase activity in the synovium of animals or in the in vitro superoxide production of neutrophils. These results suggest that rather changes in the inflammatory environment and not in the effector functions of phagocytes are responsible for the observed phenotypic and functional differences.

The cytokine IL-1β is a crucial component in the regulation of inflammatory processes, and through the activation of cyclooxygenase-2, it increases pain sensitivity as well. On the other hand, the chemokine MIP-2 is a potent chemoattractant of neutrophils (41, 127, 134, 135). Since we suspected that possibly an altered cytokine composition could be the reason of the changes in leukocyte recruitment, we chose to measure the concentration of these two compounds in the inflamed ankles- or ears of the animals. Indeed, a decreased amount of both IL-1β and MIP-2 could be detected in tissues of KO animals, which could explain why we see the reduced phagocyte numbers in ARHGAP25-deficient animals.

Since in contact hypersensitivity, T cells are crucial for disease development, we wanted to obtain a broad picture of the cytokine composition in allergen-treated animals. Thus,

cytokine array measurements were performed from the supernatants of digested ear samples. Our results show that after the first encounter with the allergen, strong expression of several interleukins could be observed in WT ears, which was absent in the KO. On the other hand, after elicitation with TNCB, interleukin levels decreased, but the expression of most CC and CXC chemokines increased in WT but not in KO animals. This data indicates that ARHGAP25 regulates the cytokine milieu in both the sensitization and the elicitation phase of the allergic reaction.

In a set of transwell experiments, we found that supernatants obtained from the ear lysate of elicited KO mice did not increase the transmigration of either WT or KO neutrophils. However, towards supernatants collected from elicited WT ears, increased migration of both WT and KO cells could be observed. These results further support our hypothesis that ARHGAP25 regulates leukocyte recruitment to the inflamed tissue through altering the cytokine milieu rather than affecting cell-autonomous migration.

Since in contact hypersensitivity, the first encounter with the allergen initiates the activation, and homing to draining lymph nodes of T cells (132), we were curious whether this process could be altered by ARHGAP25. Although the first contact with TNCB resulted in elevated cell counts and increased T cell activation in the draining lymph nodes, the absence of ARHGAP25 did not cause any alteration. When lymph node-derived cells were transferred from WT sensitized mice into KO recipients, elicitation with TNCB resulted in milder ear thickening compared to when both the donor and acceptor mice were WT, or when the donors were KO, and the acceptors were WT. These results suggest that ARHGAP25 has a more significant role in the elicitation than the sensitization of CHS. Furthermore, we conclude that the T cell homing and activation in the draining lymph nodes after sensitization are not affected by ARHGAP25.

A comprehensive western blot analysis was conducted to reveal what exact molecular mechanisms could be behind the measured decreased cytokine amounts in the absence of ARHGAP25. Investigation of the expression of different signaling proteins in the ankles of the mice revealed significantly reduced p38MAPK and I-κB levels and a decreased tendency of ERK1/2, NF-κB, E-cadherin, and β-catenin in the KO, arthritic animals compared to WT, arthritic ones. It was described that in the case of RA, in specific cell types, such as synovial fibroblasts and macrophages, increased activation of the p38MAPK pathway induces several inflammatory processes, including IL-1 and IL-6

production (32). Therefore, the inhibited p38MAPK/ERK1/2 pathway in the absence of ARHGAP25 could explain the reduced IL-1β levels in the KO animals. It was also demonstrated that NF-kB inhibits IL-1β processing and secretion in macrophages and neutrophils (42). Thus, we speculate that ARHGAP25 prevents the degradation of I-κB, which leads to the inhibited nuclear translocation of NF-κB, resulting in enhanced IL-1β production. Furthermore, we hypothesize that by activating the p38MAPK pathway and I-κB, ARHGAP25 substantially stimulates IL-1β secretion of phagocytes and fibroblast-like synoviocytes. This in turn could lead to the release of other inflammatory mediators (41, 42).

The interaction of fibroblast-like synoviocytes and CD4+ T cells promotes the release of a wide range of cytokines, such as IL-17, IL-6, IFN, TNF, and IL-1. All of these can stimulate the release of MIP-2 from macrophages, (41), which can explain the elevated levels of MIP-2 in WT animals compared to KO.

Since in recent years, the role of ARHGAP25 in non-hematopoietic cells gained focus it was imperative to reveal what other cell types could be responsible for the mitigated inflammation in the absence of ARHGAP25 (75-81). FLS is a cell type of mesenchymal origin that largely contributes to RA development and progression (10). The epithelial keratinocytes regulate both phases of CHS development (131, 132). Importantly, both cell types can promote inflammation by releasing different cytokines. Our K/BxN experiments with bone marrow chimeric animals and with reverse chimeras revealed that both the hematopoietic and the non-hematopoietic compartments contribute to the effect of ARHGAP25 in autoantibody-induced arthritis. This was demonstrated by the fact that in both types of chimeras, an intermediate decrease in the severity of inflammation and the reduction of joint function were observed. As we suspected that FLS could be a key component, we investigated the expression of ARHGAP25 in these cells. Surprisingly, we found a remarkably high, neutrophil-like expression level, which suggests that ARHGAP25 has a crucial regulatory role in FLS similar to that in neutrophils.

On the other hand, in the TNCB-induced contact hypersensitivity model, our experiments with bone marrow chimeric mice, expressing ARHGAP25 only in the hematopoietic compartment, yielded different results. In these animals, repeated exposure to the allergen substantially mitigated the inflammation, similar to that in full ARHGAP25-deficient mice. Therefore, we hypothesize that in this model, only cells of hematopoietic origin,

more precisely immune cells, are responsible for the detected differences. This was confirmed by the fact that in the isolated epidermis of the ears, we could not detect ARHGAP25 either at the mRNA or at the protein level, suggesting that keratinocytes do not express this protein, even in the elicitation phase.

Lastly, we were interested in whether ARHGAP25 expression could be altered by allergic inflammation. Both in elicited murine and dermatitic human samples, we were able to measure increased ARHGAP25 levels. This can be explained by the increased number of leukocytes in the inflamed skin or the elevated expression of ARHGAP25 in the recruited leukocytes. Based on our findings, we propose that in the future, ARHGAP25 could be a therapeutic target for inflammatory diseases. Moreover, the increase in its expression observed in human patients suffering from ACD suggests that ARHGAP25 might be used as a biomarker for contact hypersensitivity.

Taken together, we demonstrated that ARHGAP25 is essential in the pathomechanism of antibody-induced arthritis and allergic contact hypersensitivity. This protein affects the symptoms of inflammation, most likely by altering the cytokine environment and the subsequent inflammatory leukocyte invasion. We hypothesize that ARHGAP25 exerts these effects through the modulation of p38MAPK and I-κB – NF-κB signaling.

6. CONCLUSIONS

According to our objectives and the results described in detail above, our conclusions are the following:

1: ARHGAP25 is involved in the development of both autoantibody-induced arthritis and allergic contact hypersensitivity.

2: This protein is critical in the regulation of the cytokine environment and, as a result, leukocyte recruitment in inflammation.

4: In arthritis, the effect of ARHGAP25 on neutrophils and macrophages and non-immune cells, particularly FLS, are both crucial for disease development.

5: In contact hypersensitivity ARHGAP25 affects the pathomechanism through regulating only leukocytes, primarily macrophages and cytotoxic T cells.

7. SUMMARY

Although inflammatory diseases affect many people worldwide, their treatment remains limited and primarily addresses the symptoms rather than the root cause of the disease. For this reason, a deeper understanding of disease mechanisms and the identification of novel therapeutic targets are still highly necessary.

ARHGAP25 is a GTPase-activating protein that regulates the GTP-GDP cycle and thus the activity of the small G protein RAC. Our research group cloned the full-length ARHGAP25 protein and described its role in the regulation of neutrophil effector functions and leukocyte extravasation for the first time. Although initially ARHGAP25 was considered leukocyte-specific, and indeed, the expression level of this GAP is the highest in immune cells, recently, more and more publications have described its role in different types of tumors and tumor cells.

Based on these data, we hypothesized that ARHGAP25 could be a major regulatory component in inflammatory diseases, where the contribution of immune cells is extremely important. Therefore, we aimed to investigate the role of ARHGAP25 in two mechanistically distinct murine disease models of inflammation, the K/BxN serum transfer arthritis and the TNCB-induced allergic contact hypersensitivity model.

Our results demonstrate that the lack of ARHGAP25 mitigates disease severity and symptoms in both cases. In arthritis, reduced edema, pain sensitivity, and loss of articular function are associated with decreased synovial hyperplasia and cartilage destruction. In both models, the absence of ARHGAP25 resulted in decreased leukocyte recruitment and inflammatory cytokine content. During sensitization with the allergen, however, the protein had no effect on T cell homing and activation in the draining lymph nodes. Furthermore, significant ARHGAP25 expression could be detected in fibroblast-like synoviocytes. In contrast, while the expression of ARHGAP25 increased in allergic murine and human samples, it could not be detected in the epidermis. Based on these findings, complemented with our data from bone marrow chimeric mice, we conclude that ARHGAP25 likely regulates inflammation by modulating cytokine production and subsequent leukocyte recruitment. In arthritis, both immune cells and fibroblast-like synoviocytes are regulated by this protein, while in contact hypersensitivity, only cells of hematopoietic origin are affected.

ÖSSZEFOGLALÁS

A gyulladásos betegségek világszerte rengeteg embert érintenek. Ennek ellenére a terápiás lehetőségek hatékonysága még mindig korlátozott, és főként a tüneteket enyhítő gyógyszerek érhetőek el, amelyek nem szüntetik meg a betegség kiváltó okát. Ezért továbbra is nagy szükség van a betegség mechanizmusainak mélyebb megértésére és az új terápiás célpontok azonosítására.

Az ARHGAP25 egy GTPáz-aktiváló fehérje, amely a GTP-GDP-cikluson keresztül szabályozza a RAC kis G-fehérje aktivitását. Kutatócsoportunk elsőként klónozta meg a teljes hosszúságú ARHGAP25 fehérjét, és írta le a neutrofil effektor funkciók és a leukocita extravazáció szabályozásában betöltött szerepét. Ugyan kezdetben az ARHGAP25-öt leukocita specifikusnak gondolták, és az expressziós szintje valóban az immunsejtekben a legmagasabb, az utóbbi időben egyre több publikáció írja le a szerepét különböző típusú tumorokban és daganatos sejtekben.

Mind ezek alapján feltételeztük, hogy az ARHGAP25 egy fontos szabályozó fehérje lehet gyulladásos betegségekben, amelyek kialakulásában az immunsejtek rendkívül fontos szerepet töltenek be. Célul tűztük ki az ARHGAP25 szerepének vizsgálatát két patomechanizmusában nagyban különböző betegség-modell, a K/BxN szérum-transzfer arthritisz és a TNCB által kiváltott allergiás kontakt dermatitisz egérmodellekben.

Eredményeink alapján elmondhatjuk, hogy az ARHGAP25 hiánya mindkét esetben enyhíti a betegség tüneteinek súlyosságát. Artritiszben az enyhült ödéma, fájdalom érzet és ízületi funkcióvesztés, csökkent szinoviális hiperpláziával és porcpusztulással párosul. Az ARHGAP25 hiánya mindkét modellben csökkent leukocita infiltrációt és gyulladásos citokin termelést eredményezett. Az allergénnel történő szenzitizáció során azonban a fehérje nem volt hatással a T-sejtek nyirokcsomókba vándorlására és aktiválódására. Jelentős ARHGAP25-expresszió volt kimutatható a szinoviális fibroblasztokban. Ezzel szemben, ugyan az ARHGAP25 expressziója megnövekedett az allergiás egér és humán mintákban, az epidermiszben nem volt kimutatható. Ezen eredmények, valamint a csontvelő kiméra egerekkel végzett kísérleteink alapján, elmondhatjuk, hogy az ARHGAP25 valószínűleg a citokintermelés és azzal együtt járó leukocita toborzás modulálásán keresztül súlyosbítja a gyulladást. Arthritisben mind az immunsejteket, mind a szinoviális fibroblasztokat, míg kontakt dermatitiszben nagy valószínűséggel csak a leukocitákat szabályozza ez a fehérje.

8. REFERENCES

1. Wu D, Luo Y, Li T, Zhao X, Lv T, Fang G, et al. Systemic complications of rheumatoid arthritis: Focus on pathogenesis and treatment. Front Immunol. 2022;13:1051082.

2. O'Neil LJ, Kaplan MJ. Neutrophils in Rheumatoid Arthritis: Breaking Immune Tolerance and Fueling Disease. Trends Mol Med. 2019;25(3):215-27.

3. Lin YJ, Anzaghe M, Schulke S. Update on the Pathomechanism, Diagnosis, and Treatment Options for Rheumatoid Arthritis. Cells. 2020;9(4).

4. Macfarlane E, Seibel MJ, Zhou H. Arthritis and the role of endogenous glucocorticoids. Bone Res. 2020;8:33.

5. Sokolove J, Bromberg R, Deane KD, Lahey LJ, Derber LA, Chandra PE, et al. Autoantibody epitope spreading in the pre-clinical phase predicts progression to rheumatoid arthritis. PLoS One. 2012;7(5):e35296.

6. Smolen JS, Aletaha D. The challenge of following process, damage, and function in patients with rheumatoid arthritis in clinical care. Curr Rheumatol Rep. 2003;5(5):336-40.

7. Livshits G, Kalinkovich A. Hierarchical, imbalanced pro-inflammatory cytokine networks govern the pathogenesis of chronic arthropathies. Osteoarthritis Cartilage. 2018;26(1):7-17.

8. Garcia-Hernandez MH, Gonzalez-Amaro R, Portales-Perez DP. Specific therapy to regulate inflammation in rheumatoid arthritis: molecular aspects. Immunotherapy. 2014;6(5):623-36.

9. Wright HL, Moots RJ, Edwards SW. The multifactorial role of neutrophils in rheumatoid arthritis. Nat Rev Rheumatol. 2014;10(10):593-601.

10. Lefevre S, Knedla A, Tennie C, Kampmann A, Wunrau C, Dinser R, et al. Synovial fibroblasts spread rheumatoid arthritis to unaffected joints. Nat Med. 2009;15(12):1414-20.

11. Gravallese EM, Firestein GS. Rheumatoid Arthritis - Common Origins, Divergent Mechanisms. N Engl J Med. 2023;388(6):529-42.

12. Caplazi P, Baca M, Barck K, Carano RA, DeVoss J, Lee WP, et al. Mouse Models of Rheumatoid Arthritis. Vet Pathol. 2015;52(5):819-26.

13. Alfonso JH, Bauer A, Bensefa-Colas L, Boman A, Bubas M, Constandt L, et al. Minimum standards on prevention, diagnosis and treatment of occupational and work-related skin diseases in Europe - position paper of the COST Action StanDerm (TD 1206). J Eur Acad Dermatol Venereol. 2017;31 Suppl 4:31-43.

14. Mowad CM, Anderson B, Scheinman P, Pootongkam S, Nedorost S, Brod B. Allergic contact dermatitis: Patient management and education. J Am Acad Dermatol. 2016;74(6):1043-54.

15. Adam C, Wohlfarth J, Haussmann M, Sennefelder H, Rodin A, Maler M, et al. Allergy-Inducing Chromium Compounds Trigger Potent Innate Immune Stimulation Via ROS-Dependent Inflammasome Activation. J Invest Dermatol. 2017;137(2):367-76.

16. Toebak MJ, Gibbs S, Bruynzeel DP, Scheper RJ, Rustemeyer T. Dendritic cells: biology of the skin. Contact Dermatitis. 2009;60(1):2-20.

17. Romani N, Clausen BE, Stoitzner P. Langerhans cells and more: langerin-expressing dendritic cell subsets in the skin. Immunol Rev. 2010;234(1):120-41.

18. Komori HK, Witherden DA, Kelly R, Sendaydiego K, Jameson JM, Teyton L, et al. Cutting edge: dendritic epidermal gammadelta T cell ligands are rapidly and locally expressed by keratinocytes following cutaneous wounding. J Immunol. 2012;188(7):2972-6.

19. Shabgah AG, Fattahi E, Shahneh FZ. Interleukin-17 in human inflammatory diseases. Postepy Dermatol Alergol. 2014;31(4):256-61.

20. Silvestre MC, Reis V. Evaluation of the profile of inflammatory cytokines, through immunohistochemistry, in the skin of patients with allergic contact dermatitis to nickel in the acute and chronic phases. An Bras Dermatol. 2018;93(6):829-35.

21. Gocinski BL, Tigelaar RE. Roles of CD4+ and CD8+ T cells in murine contact sensitivity revealed by in vivo monoclonal antibody depletion. J Immunol. 1990;144(11):4121-8.

22. Bour H, Peyron E, Gaucherand M, Garrigue JL, Desvignes C, Kaiserlian D, et al. Major histocompatibility complex class I-restricted CD8+ T cells and class II-restricted CD4+ T cells, respectively, mediate and regulate contact sensitivity to dinitrofluorobenzene. Eur J Immunol. 1995;25(11):3006-10.

23. Schmidt M, Goebeler M. Immunology of metal allergies. J Dtsch Dermatol Ges. 2015;13(7):653-60.

24. Buters J, Biedermann T. Chromium(VI) Contact Dermatitis: Getting Closer to Understanding the Underlying Mechanisms of Toxicity and Sensitization! J Invest Dermatol. 2017;137(2):274-7.

25. Weber FC, Nemeth T, Csepregi JZ, Dudeck A, Roers A, Ozsvari B, et al. Neutrophils are required for both the sensitization and elicitation phase of contact hypersensitivity. J Exp Med. 2015;212(1):15-22.

26. Kobayashi Y. The role of chemokines in neutrophil biology. Front Biosci. 2008;13:2400-7.

27. Carbone T, Nasorri F, Pennino D, Donnarumma M, Garcovich S, Eyerich K, et al. CD56 highCD16 - NK cell involvement in cutaneous lichen planus. Eur J Dermatol. 2010;20(6):724-30.

28. O'Leary JG, Goodarzi M, Drayton DL, von Andrian UH. T cell- and B cell-independent adaptive immunity mediated by natural killer cells. Nat Immunol. 2006;7(5):507-16.

29. Azeem M, Kader H, Kerstan A, Hetta HF, Serfling E, Goebeler M, et al. Intricate Relationship Between Adaptive and Innate Immune System in Allergic Contact Dermatitis. Yale J Biol Med. 2020;93(5):699-709.

30. Yong HY, Koh MS, Moon A. The p38 MAPK inhibitors for the treatment of inflammatory diseases and cancer. Expert Opin Investig Drugs. 2009;18(12):1893-905.

31. Johnson GL, Lapadat R. Mitogen-activated protein kinase pathways mediated by ERK, JNK, and p38 protein kinases. Science. 2002;298(5600):1911-2.

32. Schett G, Zwerina J, Firestein G. The p38 mitogen-activated protein kinase (MAPK) pathway in rheumatoid arthritis. Ann Rheum Dis. 2008;67(7):909-16.

33. Holgate ST. Cytokine and anti-cytokine therapy for the treatment of asthma and allergic disease. Cytokine. 2004;28(4-5):152-7.

34. Williams RO, Paleolog E, Feldmann M. Cytokine inhibitors in rheumatoid arthritis and other autoimmune diseases. Curr Opin Pharmacol. 2007;7(4):412-7.

35. Chung KF. Cytokines as targets in chronic obstructive pulmonary disease. Curr Drug Targets. 2006;7(6):675-81.

36. Chen LW, Egan L, Li ZW, Greten FR, Kagnoff MF, Karin M. The two faces of IKK and NF-kappaB inhibition: prevention of systemic inflammation but increased local injury following intestinal ischemia-reperfusion. Nat Med. 2003;9(5):575-81.

37. Eckmann L, Nebelsiek T, Fingerle AA, Dann SM, Mages J, Lang R, et al. Opposing functions of IKKbeta during acute and chronic intestinal inflammation. Proc Natl Acad Sci U S A. 2008;105(39):15058-63.

38. Poynter ME, Irvin CG, Janssen-Heininger YM. A prominent role for airway epithelial NF-kappa B activation in lipopolysaccharide-induced airway inflammation. J Immunol. 2003;170(12):6257-65.

39. Kang J, Song J, Shen S, Li B, Yang X, Chen M. Diisononyl phthalate aggravates allergic dermatitis by activation of NF-kB. Oncotarget. 2016;7(51):85472-82.

40. Lawrence T, Gilroy DW, Colville-Nash PR, Willoughby DA. Possible new role for NF-kappaB in the resolution of inflammation. Nat Med. 2001;7(12):1291-7.

41. Yang J, Wang J, Liang X, Zhao H, Lu J, Ma Q, et al. IL-1beta increases the expression of inflammatory factors in synovial fluid-derived fibroblast-like synoviocytes via activation of the NF-kappaB-mediated ERK-STAT1 signaling pathway. Mol Med Rep. 2019;20(6):4993-5001.

42. Greten FR, Arkan MC, Bollrath J, Hsu LC, Goode J, Miething C, et al. NF-kappaB is a negative regulator of IL-1beta secretion as revealed by genetic and pharmacological inhibition of IKKbeta. Cell. 2007;130(5):918-31.

43. Beg AA, Baltimore D. An essential role for NF-kappaB in preventing TNF-alpha-induced cell death. Science. 1996;274(5288):782-4.

44. Lawrence T, Gilroy DW. Chronic inflammation: a failure of resolution? Int J Exp Pathol. 2007;88(2):85-94.

45. Dou C, Yan Y, Dong S. Role of cadherin-11 in synovial joint formation and rheumatoid arthritis pathology. Mod Rheumatol. 2013;23(6):1037-44.

46. Shiohara T, Hayakawa J, Mizukawa Y. Animal models for atopic dermatitis: are they relevant to human disease? J Dermatol Sci. 2004;36(1):1-9.

47. Kouskoff V, Korganow AS, Duchatelle V, Degott C, Benoist C, Mathis D. Organ-specific disease provoked by systemic autoimmunity. Cell. 1996;87(5):811-22.

48. Ditzel HJ. The K/BxN mouse: a model of human inflammatory arthritis. Trends Mol Med. 2004;10(1):40-5.

49. Korganow AS, Weber JC, Martin T. [Animal models and autoimmune diseases]. Rev Med Interne. 1999;20(3):283-6.

50. Mangialaio S, Ji H, Korganow AS, Kouskoff V, Benoist C, Mathis D. The arthritogenic T cell receptor and its ligand in a model of spontaneous arthritis. Arthritis Rheum. 1999;42(12):2517-23.

51. Ji H, Gauguier D, Ohmura K, Gonzalez A, Duchatelle V, Danoy P, et al. Genetic influences on the end-stage effector phase of arthritis. J Exp Med. 2001;194(3):321-30.

52. Safi S, Frommholz D, Reimann S, Gotz W, Bourauel C, Neumann AL, et al. Comparative study on serum-induced arthritis in the temporomandibular and limb joint of mice. Int J Rheum Dis. 2019;22(4):636-45.

53. Matsumoto I, Maccioni M, Lee DM, Maurice M, Simmons B, Brenner M, et al. How antibodies to a ubiquitous cytoplasmic enzyme may provoke joint-specific autoimmune disease. Nat Immunol. 2002;3(4):360-5.

54. Maccioni M, Zeder-Lutz G, Huang H, Ebel C, Gerber P, Hergueux J, et al. Arthritogenic monoclonal antibodies from K/BxN mice. J Exp Med. 2002;195(8):1071-7.

55. Wipke BT, Wang Z, Nagengast W, Reichert DE, Allen PM. Staging the initiation of autoantibody-induced arthritis: a critical role for immune complexes. J Immunol. 2004;172(12):7694-702.

56. Corr M, Crain B. The role of FcgammaR signaling in the K/B x N serum transfer model of arthritis. J Immunol. 2002;169(11):6604-9.

57. Chou RC, Kim ND, Sadik CD, Seung E, Lan Y, Byrne MH, et al. Lipid-cytokine-chemokine cascade drives neutrophil recruitment in a murine model of inflammatory arthritis. Immunity. 2010;33(2):266-78.

58. Christensen AD, Haase C, Cook AD, Hamilton JA. K/BxN Serum-Transfer Arthritis as a Model for Human Inflammatory Arthritis. Front Immunol. 2016;7:213.

59. Blom AB, van Lent PL, van Vuuren H, Holthuysen AE, Jacobs C, van de Putte LB, et al. Fc gamma R expression on macrophages is related to severity and chronicity of synovial inflammation and cartilage destruction during experimental immune-complex-mediated arthritis (ICA). Arthritis Res. 2000;2(6):489-503.

60. Solomon S, Rajasekaran N, Jeisy-Walder E, Snapper SB, Illges H. A crucial role for macrophages in the pathology of K/B x N serum-induced arthritis. Eur J Immunol. 2005;35(10):3064-73.

61. Misharin AV, Cuda CM, Saber R, Turner JD, Gierut AK, Haines GK, 3rd, et al. Nonclassical Ly6C(-) monocytes drive the development of inflammatory arthritis in mice. Cell Rep. 2014;9(2):591-604.

62. Cook AD, Turner AL, Braine EL, Pobjoy J, Lenzo JC, Hamilton JA. Regulation of systemic and local myeloid cell subpopulations by bone marrow cell-derived granulocyte-macrophage colony-stimulating factor in experimental inflammatory arthritis. Arthritis Rheum. 2011;63(8):2340-51.

63. Pettit AR, Ji H, von Stechow D, Muller R, Goldring SR, Choi Y, et al. TRANCE/RANKL knockout mice are protected from bone erosion in a serum transfer model of arthritis. Am J Pathol. 2001;159(5):1689-99.

64. Ji H, Pettit A, Ohmura K, Ortiz-Lopez A, Duchatelle V, Degott C, et al. Critical roles for interleukin 1 and tumor necrosis factor alpha in antibody-induced arthritis. J Exp Med. 2002;196(1):77-85.

65. Firestein GS. Evolving concepts of rheumatoid arthritis. Nature. 2003;423(6937):356-61.

66. Csepanyi-Komi R, Levay M, Ligeti E. Small G proteins and their regulators in cellular signalling. Mol Cell Endocrinol. 2012;353(1-2):10-20.

67. Csepanyi-Komi R, Pasztor M, Bartos B, Ligeti E. The neglected terminators: Rho family GAPs in neutrophils. Eur J Clin Invest. 2018;48 Suppl 2:e12993.

68. Csepanyi-Komi R, Sirokmany G, Geiszt M, Ligeti E. ARHGAP25, a novel Rac GTPase-activating protein, regulates phagocytosis in human neutrophilic granulocytes. Blood. 2012;119(2):573-82.

69. Lorincz AM, Szarvas G, Smith SM, Ligeti E. Role of Rac GTPase activating proteins in regulation of NADPH oxidase in human neutrophils. Free Radic Biol Med. 2014;68:65-71.

70. Csepanyi-Komi R, Wisniewski E, Bartos B, Levai P, Nemeth T, Balazs B, et al. Rac GTPase Activating Protein ARHGAP25 Regulates Leukocyte Transendothelial Migration in Mice. J Immunol. 2016;197(7):2807-15.

71. Wang LD, Ficarro SB, Hutchinson JN, Csepanyi-Komi R, Nguyen PT, Wisniewski E, et al. Phosphoproteomic profiling of mouse primary HSPCs reveals new regulators of HSPC mobilization. Blood. 2016;128(11):1465-74.

72. Wisniewski E, Czaran D, Kovacs F, Bahurek E, Nemeth A, Sasvari P, et al. A novel BRET-Based GAP assay reveals phosphorylation-dependent regulation of the RAC-specific GTPase activating protein ARHGAP25. FASEB J. 2022;36(11):e22584.

73. Lindner SE, Egelston CA, Huard SM, Lee PP, Wang LD. Arhgap25 Deficiency Leads to Decreased Numbers of Peripheral Blood B Cells and Defective Germinal Center Reactions. Immunohorizons. 2020;4(5):274-81.

74. Thuault S, Comunale F, Hasna J, Fortier M, Planchon D, Elarouci N, et al. The RhoE/ROCK/ARHGAP25 signaling pathway controls cell invasion by inhibition of Rac activity. Mol Biol Cell. 2016;27(17):2653-61.

75. Tao L, Zhu Y, Gu Y, Zheng J, Yang J. ARHGAP25: A negative regulator of colorectal cancer (CRC) metastasis via the Wnt/beta-catenin pathway. Eur J Pharmacol. 2019;858:172476.

76. Tao L, Gu Y, Zheng J, Yang J, Zhu Y. Weichang'an suppressed migration and invasion of HCT116 cells by inhibiting Wnt/beta-catenin pathway while upregulating ARHGAP25. Biotechnol Appl Biochem. 2019;66(5):787-93.

77. Xu K, Liu B, Ma Y. The tumor suppressive roles of ARHGAP25 in lung cancer cells. Onco Targets Ther. 2019;12:6699-710.

78. Shi F, Wu J, Jia Q, Li K, Li W, Shi Y, et al. Relationship between the expression of ARHGAP25 and RhoA in non-small cell lung cancer and vasculogenic mimicry. BMC Pulm Med. 2022;22(1):377.

79. Han S, Jin X, Hu T, Chi F. ARHGAP25 suppresses the development of breast cancer by an ARHGAP25/Wnt/ASCL2 feedback loop. Carcinogenesis. 2023;44(5):369-82.

80. Huang WK, Chen Y, Su H, Chen TY, Gao J, Liu Y, et al. ARHGAP25 Inhibits Pancreatic Adenocarcinoma Growth by Suppressing Glycolysis via AKT/mTOR Pathway. Int J Biol Sci. 2021;17(7):1808-20.

81. Zhang Y, Lin Y, Zhu Y, Zhang X, Tao L, Yang M. ARHGAP25 expression in colorectal cancer as a biomarker associated with favorable prognosis. Mol Clin Oncol. 2022;16(4):84.

82. Makitie RE, Henning P, Jiu Y, Kampe A, Kogan K, Costantini A, et al. An ARHGAP25 variant links aberrant Rac1 function to early-onset skeletal fragility. JBMR Plus. 2021;5(7):e10509.

83. Hou Y, Xie Y, Liu X, Chen Y, Zhou F, Yang B. Oxygen glucose deprivation-pretreated astrocyte-derived exosomes attenuates intracerebral hemorrhage (ICH)-induced BBB disruption through miR-27a-3p /ARHGAP25/Wnt/beta-catenin axis. Fluids Barriers CNS. 2024;21(1):8.

84. Sasvari P, Pettko-Szandtner A, Wisniewski E, Csepanyi-Komi R. Neutrophil-specific interactome of ARHGAP25 reveals novel partners and regulatory insights. Sci Rep. 2024;14(1):20106.

85. O'Dell JR. Therapeutic strategies for rheumatoid arthritis. N Engl J Med. 2004;350(25):2591-602.

86. Chiba T, Sato K, Endo M, Ando T, Inomata M, Orii S, et al. Upper gastrointestinal disorders induced by non-steroidal anti-inflammatory drugs. Hepatogastroenterology. 2005;52(64):1134-8.

87. Guidelines for monitoring drug therapy in rheumatoid arthritis. American College of Rheumatology Ad Hoc Committee on Clinical Guidelines. Arthritis Rheum. 1996;39(5):723-31.

88. Lisse JR, Perlman M, Johansson G, Shoemaker JR, Schechtman J, Skalky CS, et al. Gastrointestinal tolerability and effectiveness of rofecoxib versus naproxen in the treatment of osteoarthritis: a randomized, controlled trial. Ann Intern Med. 2003;139(7):539-46.

89. Bombardier C, Laine L, Reicin A, Shapiro D, Burgos-Vargas R, Davis B, et al. Comparison of upper gastrointestinal toxicity of rofecoxib and naproxen in patients with rheumatoid arthritis. VIGOR Study Group. N Engl J Med. 2000;343(21):1520-8, 2 p following 8.

90. Buttgereit F, Straub RH, Wehling M, Burmester GR. Glucocorticoids in the treatment of rheumatic diseases: an update on the mechanisms of action. Arthritis Rheum. 2004;50(11):3408-17.

91. Spies CM, Bijlsma JW, Burmester GR, Buttgereit F. Pharmacology of glucocorticoids in rheumatoid arthritis. Curr Opin Pharmacol. 2010;10(3):302-7.

92. Quemeneur L, Gerland LM, Flacher M, Ffrench M, Revillard JP, Genestier L. Differential control of cell cycle, proliferation, and survival of primary T lymphocytes by purine and pyrimidine nucleotides. J Immunol. 2003;170(10):4986-95.

93. Cronstein BN. Low-dose methotrexate: a mainstay in the treatment of rheumatoid arthritis. Pharmacol Rev. 2005;57(2):163-72.

94. Montesinos MC, Desai A, Delano D, Chen JF, Fink JS, Jacobson MA, et al. Adenosine A2A or A3 receptors are required for inhibition of inflammation by methotrexate and its analog MX-68. Arthritis Rheum. 2003;48(1):240-7.

95. Gadangi P, Longaker M, Naime D, Levin RI, Recht PA, Montesinos MC, et al. The anti-inflammatory mechanism of sulfasalazine is related to adenosine release at inflamed sites. J Immunol. 1996;156(5):1937-41.

96. Fox RI, Kang HI. Mechanism of action of antimalarial drugs: inhibition of antigen processing and presentation. Lupus. 1993;2 Suppl 1:S9-12.

97. Weber SM, Levitz SM. Chloroquine interferes with lipopolysaccharide-induced TNF-alpha gene expression by a nonlysosomotropic mechanism. J Immunol. 2000;165(3):1534-40.

98. Kremer JM. Methotrexate and leflunomide: biochemical basis for combination therapy in the treatment of rheumatoid arthritis. Semin Arthritis Rheum. 1999;29(1):14-26.

99. Elliott MJ, Maini RN, Feldmann M, Long-Fox A, Charles P, Katsikis P, et al. Treatment of rheumatoid arthritis with chimeric monoclonal antibodies to tumor necrosis factor alpha. Arthritis Rheum. 1993;36(12):1681-90.

100. Voulgari PV, Drosos AA. Adalimumab for rheumatoid arthritis. Expert Opin Biol Ther. 2006;6(12):1349-60.

101. Nestorov I. Clinical pharmacokinetics of TNF antagonists: how do they differ? Semin Arthritis Rheum. 2005;34(5 Suppl1):12-8.

102. Sany J, Kaiser MJ, Jorgensen C, Trape G. Study of the tolerance of infliximab infusions with or without betamethasone premedication in patients with active rheumatoid arthritis. Ann Rheum Dis. 2005;64(11):1647-9.

103. Bongartz T, Sutton AJ, Sweeting MJ, Buchan I, Matteson EL, Montori V. Anti-TNF antibody therapy in rheumatoid arthritis and the risk of serious infections and

malignancies: systematic review and meta-analysis of rare harmful effects in randomized controlled trials. JAMA. 2006;295(19):2275-85.

104. Cron RQ. A signal achievement in the treatment of arthritis. Arthritis Rheum. 2005;52(8):2229-32.

105. Cross AH, Stark JL, Lauber J, Ramsbottom MJ, Lyons JA. Rituximab reduces B cells and T cells in cerebrospinal fluid of multiple sclerosis patients. J Neuroimmunol. 2006;180(1-2):63-70.

106. Schett G, Tohidast-Akrad M, Smolen JS, Schmid BJ, Steiner CW, Bitzan P, et al. Activation, differential localization, and regulation of the stress-activated protein kinases, extracellular signal-regulated kinase, c-JUN N-terminal kinase, and p38 mitogen-activated protein kinase, in synovial tissue and cells in rheumatoid arthritis. Arthritis Rheum. 2000;43(11):2501-12.

107. Gabay C, Riek M, Scherer A, Finckh A, physicians Sc. Effectiveness of biologic DMARDs in monotherapy versus in combination with synthetic DMARDs in rheumatoid arthritis: data from the Swiss Clinical Quality Management Registry. Rheumatology (Oxford). 2015;54(9):1664-72.

108. Lopez-Santalla M, Fernandez-Perez R, Garin MI. Mesenchymal Stem/Stromal Cells for Rheumatoid Arthritis Treatment: An Update on Clinical Applications. Cells. 2020;9(8).

109. Moghaddam MZ, Mousavi MJ, Ghotloo S. Cell-based therapies for the treatment of rheumatoid arthritis. Immun Inflamm Dis. 2023;11(11):e1091.

110. Scheinman PL, Vocanson M, Thyssen JP, Johansen JD, Nixon RL, Dear K, et al. Contact dermatitis. Nat Rev Dis Primers. 2021;7(1):38.

111. Coondoo A, Phiske M, Verma S, Lahiri K. Side-effects of topical steroids: A long overdue revisit. Indian Dermatol Online J. 2014;5(4):416-25.

112. Han JS, Won KH, Chang SE, Kim JE. Tacrolimus 0.1% ointment in the treatment of allergic contact dermatitis: a new approach. Int J Dermatol. 2014;53(10):e470-1.

113. Bauer A, Thyssen JP, Buhl T, Nielsen TSS, Larsen LS, Osterskov AB, et al. Treatment with delgocitinib cream improves itch, pain and other signs and symptoms of chronic hand eczema: Results from the Hand Eczema Symptom Diary in a phase IIb randomized clinical trial. Contact Dermatitis. 2023;89(1):46-53.

114. Bissonnette R, Warren RB, Pinter A, Agner T, Gooderham M, Schuttelaar MLA, et al. Efficacy and safety of delgocitinib cream in adults with moderate to severe chronic hand eczema (DELTA 1 and DELTA 2): results from multicentre, randomised, controlled, double-blind, phase 3 trials. Lancet. 2024;404(10451):461-73.

115. Patel A, Burns E, Burkemper NM. Methotrexate use in allergic contact dermatitis: a retrospective study. Contact Dermatitis. 2018;78(3):194-8.

116. Cassano N, Loconsole F, Coviello C, Vena GA. Infliximab in recalcitrant severe atopic eczema associated with contact allergy. Int J Immunopathol Pharmacol. 2006;19(1):237-40.

117. Chipalkatti N, Lee N, Zancanaro P, Dumont N, Donovan C, Rosmarin D. Dupilumab as a Treatment for Allergic Contact Dermatitis. Dermatitis. 2018;29(6):347-8.

118. Koh YG, Park JW, Shin SH, Kim BJ, Yoo KH. Dupilumab for the treatment of refractory allergic contact dermatitis from rubber/latex concomitant with atopic dermatitis. J Eur Acad Dermatol Venereol. 2022;36(8):e640-e3.

119. Kovacs M, Nemeth T, Jakus Z, Sitaru C, Simon E, Futosi K, et al. The Src family kinases Hck, Fgr, and Lyn are critical for the generation of the in vivo inflammatory environment without a direct role in leukocyte recruitment. J Exp Med. 2014;211(10):1993-2011.

120. Jakus Z, Simon E, Frommhold D, Sperandio M, Mocsai A. Critical role of phospholipase Cgamma2 in integrin and Fc receptor-mediated neutrophil functions and the effector phase of autoimmune arthritis. J Exp Med. 2009;206(3):577-93.

121. Batai IZ, Sar CP, Horvath A, Borbely E, Bolcskei K, Kemeny A, et al. TRPA1 Ion Channel Determines Beneficial and Detrimental Effects of GYY4137 in Murine Serum-Transfer Arthritis. Front Pharmacol. 2019;10:964.

122. Szabo A, Helyes Z, Sandor K, Bite A, Pinter E, Nemeth J, et al. Role of transient receptor potential vanilloid 1 receptors in adjuvant-induced chronic arthritis: in vivo study using gene-deficient mice. J Pharmacol Exp Ther. 2005;314(1):111-9.

123. Gross S, Gammon ST, Moss BL, Rauch D, Harding J, Heinecke JW, et al. Bioluminescence imaging of myeloperoxidase activity in vivo. Nat Med. 2009;15(4):455-61.

124. Tseng JC, Kung AL. In vivo imaging of inflammatory phagocytes. Chem Biol. 2012;19(9):1199-209.

125. Yang TT, Sinai P, Kain SR. An acid phosphatase assay for quantifying the growth of adherent and nonadherent cells. Anal Biochem. 1996;241(1):103-8.

126. Nemeth T, Futosi K, Sitaru C, Ruland J, Mocsai A. Neutrophil-specific deletion of the CARD9 gene expression regulator suppresses autoantibody-induced inflammation in vivo. Nat Commun. 2016;7:11004.

127. Futosi K, Kasa O, Szilveszter KP, Mocsai A. Neutrophil Phospholipase Cgamma2 Drives Autoantibody-Induced Arthritis Through the Generation of the Inflammatory Microenvironment. Arthritis Rheumatol. 2021;73(9):1614-25.

128. Gabay C, Lamacchia C, Palmer G. IL-1 pathways in inflammation and human diseases. Nat Rev Rheumatol. 2010;6(4):232-41.

129. Szilveszter KP, Vikar S, Horvath AI, Helyes Z, Sardy M, Mocsai A. Phospholipase Cgamma2 Is Essential for Experimental Models of Epidermolysis Bullosa Acquisita. J Invest Dermatol. 2022;142(4):1114-25.

130. Adamczyk M, Bartosinska J, Raczkiewicz D, Kowal M, Surdacka A, Krasowska D, et al. The Expression of Activation Markers CD25 and CD69 Increases during Biologic Treatment of Psoriasis. J Clin Med. 2023;12(20).

131. Martin SF, Jakob T. From innate to adaptive immune responses in contact hypersensitivity. Curr Opin Allergy Clin Immunol. 2008;8(4):289-93.

132. Martin SF. Immunological mechanisms in allergic contact dermatitis. Curr Opin Allergy Clin Immunol. 2015;15(2):124-30.

133. Mittal M, Siddiqui MR, Tran K, Reddy SP, Malik AB. Reactive oxygen species in inflammation and tissue injury. Antioxid Redox Signal. 2014;20(7):1126-67.

134. Kim DS, Han JH, Kwon HJ. NF-kappaB and c-Jun-dependent regulation of macrophage inflammatory protein-2 gene expression in response to lipopolysaccharide in RAW 264.7 cells. Mol Immunol. 2003;40(9):633-43.

135. Ren K, Torres R. Role of interleukin-1beta during pain and inflammation. Brain Res Rev. 2009;60(1):57-64.

9. BIBLIOGRAPHY OF THE CANDIDATE'S PUBLICATIONS

Candidate's publications related to the work discussed in this thesis

Czárán, Domonkos; Sasvári, Péter; Horváth, Ádám István; Ella, Krisztina; Réka Sűdy, Ágnes; Borbely, Eva; Rusznák, Kitti; Czéh, Boldizsár; Mócsai, Attila; Helyes, Zsuzsanna
Lacking ARHGAP25 mitigates the symptoms of autoantibody-induced arthritis in mice
FRONTIERS IN IMMUNOLOGY 14 Paper: 1182278, 13 p. (2023)
IF: 5,7
DOI: 10.3389/fimmu.2023.1182278

Czárán D, Sasvári P, Lőrincz K, Ella K, Gellén V, Csépányi-Kömi R.
ARHGAP25: a novel player in the Pathomechanism of allergic contact hypersensitivity.
FRONTIERS IN IMMUNOLOGY 26; 16:1509713. (2025)
IF: 5,9
DOI: 10.3389/fimmu.2025.1509713.

Candidate's publications unrelated to the work discussed in this thesis

Wisniewski, Éva; **Czárán, Domonkos***; Kovács, Fanni; Bahurek, Enikő; Németh, Afrodité; Sasvári, Péter; Szanda, Gergő; Pettkó-Szandtner, Aladár; Klement, Eva; Ligeti, Erzsébet
A Novel BRET-Based GAP assay reveals phosphorylation-dependent regulation of the RAC-specific GTPase activating protein ARHGAP25
FASEB JOURNAL 36: 11 Paper: e22584, 19 p. (2022)
*Éva Wisniewski and Domonkos Czárán should be considered joint first authors.
IF: 4,8
DOI: 10.1096/fj.202200689R

Szederkényi, G; Kocsis, D; Vághy, M A; **Czárán, D**; Sasvári, P; Lengyel, M; Naszlady, M B; Kreis, F; Antal, I; Csépányi-Kömi, R
Mathematical modeling of transdermal delivery of topical drug formulations in a dynamic microfluidic diffusion chamber in health and disease
PLOS ONE 19: 4 Paper: 0299501 , 17 p. (2024)
IF: 2,6
DOI: 10.1371/journal.pone.0299501

Kovács F, Posvai T, Zsáry E, Kolonics F, Garai R, Herczeg V, **Czárán D**, Takács J, Szabó AJ, Krivácsy P, Csépányi-Kömi R.

Long COVID syndrome in children: neutrophilic granulocyte dysfunction and its correlation with disease severity.

PEDIATRIC RESEARCH Nov 27. 13 p. (2024)

IF: 3,1

DOI: 10.1038/s41390-024-03731-1.

10. ACKNOWLEDGEMENTS

I am sincerely thankful to my supervisor Dr. Roland Csépányi-Kömi for his careful guidance, and countless valuable advice through my PhD studies. I am also grateful to Professor Erzsébet Ligeti, former leader of our research group, for giving me the chance to work in this excellent lab, and for her immense professional help, especially in the first half of my PhD studies.

I owe gratitude to Professor Attila Mócsai and Professor László Hunyady, current and former heads of the Department of Physiology, and Professor Péter Enyedi, chairman of the Molecular Medicine Doctoral School, for giving me the opportunity to conduct my PhD research in this friendly and academically inspiring environment.

I am indebted to my colleagues in the Department of Physiology, and especially to my colleagues in the Phagocyte Physiology research group: Dr. Péter Sasvári, Dr. Éva Wisniewski, Mátka Nagy, Dr Viktória Szeifert, Dr. Csaba Tímár, Dr Márton Ákos Lőrincz and Renáta Bíró who helped me greatly with insightful advice, encouraging words and actual deeds.

I owe a special thanks to Regina Tóth-Kun for her professional and precise technical assistance in the preparation and execution of my experiments, and for her friendly and approachable attitude which made our lab a great workplace.

Last but not least, I would like to express my appreciation to my family who supported me every way they could throughout my studies.